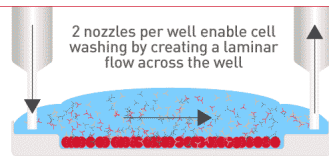


Check out how Laminar Wash systems replace centrifugation completely in handling cells



See How It Works



Cytomegalovirus (CMV) Epitope-Specific CD4⁺ T Cells Are Inflated in HIV⁺ CMV⁺ Subjects

This information is current as of June 28, 2019.

Chike O. Abana, Mark A. Pilkinton, Silvana Gaudieri, Abha Chopra, Wyatt J. McDonnell, Celestine Wanjalla, Louise Barnett, Rama Gangula, Cindy Hager, Dae K. Jung, Brian G. Engelhardt, Madan H. Jagasia, Paul Klenerman, Elizabeth J. Phillips, David M. Koelle, Spyros A. Kalams and Simon A. Mallal

J Immunol published online 2 October 2017
<http://www.jimmunol.org/content/early/2017/09/29/jimmunol.1700851>

Supplementary Material <http://www.jimmunol.org/content/suppl/2017/09/29/jimmunol.1700851.DCSupplemental>

Why *The JI*? Submit online.

- **Rapid Reviews!** 30 days* from submission to initial decision
- **No Triage!** Every submission reviewed by practicing scientists
- **Fast Publication!** 4 weeks from acceptance to publication

*average

Subscription Information about subscribing to *The Journal of Immunology* is online at:
<http://jimmunol.org/subscription>

Permissions Submit copyright permission requests at:
<http://www.aai.org/About/Publications/JI/copyright.html>

Email Alerts Receive free email-alerts when new articles cite this article. Sign up at:
<http://jimmunol.org/alerts>



Cytomegalovirus (CMV) Epitope-Specific CD4⁺ T Cells Are Inflated in HIV⁺ CMV⁺ Subjects

Chike O. Abana,* Mark A. Pilkinton,[†] Silvana Gaudieri,^{†,‡,§} Abha Chopra,[§] Wyatt J. McDonnell,* Celestine Wanjalla,[†] Louise Barnett,[†] Rama Gangula,[†] Cindy Hager,[†] Dae K. Jung,[¶] Brian G. Engelhardt,[¶] Madan H. Jagasia,[¶] Paul Klenerman,^{||} Elizabeth J. Phillips,^{*,†,§} David M. Koelle,[#] Spyros A. Kalams,^{*,†,1} and Simon A. Mallal*,^{†,§,1}

Select CMV epitopes drive life-long CD8⁺ T cell memory inflation, but the extent of CD4 memory inflation is poorly studied. CD4⁺ T cells specific for human CMV (HCMV) are elevated in HIV⁺ HCMV⁺ subjects. To determine whether HCMV epitope-specific CD4⁺ T cell memory inflation occurs during HIV infection, we used HLA-DR7 (DRB1*07:01) tetramers loaded with the glycoprotein B DYSNTHSTRYV (DYS) epitope to characterize circulating CD4⁺ T cells in coinfecting HLA-DR7⁺ long-term non-progressor HIV subjects with undetectable HCMV plasma viremia. DYS-specific CD4⁺ T cells were inflated among these HIV⁺ subjects compared with those from an HIV⁻ HCMV⁺ HLA-DR7⁺ cohort or with HLA-DR7-restricted CD4⁺ T cells from the HIV-coinfected cohort that were specific for epitopes of HCMV phosphoprotein-65, tetanus toxoid precursor, EBV nuclear Ag 2, or HIV gag protein. Inflated DYS-specific CD4⁺ T cells consisted of effector memory or effector memory-RA⁺ subsets with restricted TCR β usage and nearly monoclonal CDR3 containing novel conserved amino acids. Expression of this near-monoclonal TCR in a Jurkat cell-transfection system validated fine DYS specificity. Inflated cells were polyfunctional, not senescent, and displayed high ex vivo levels of granzyme B, CX₃CR1, CD38, or HLA-DR but less often coexpressed CD38⁺ and HLA-DR⁺. The inflation mechanism did not involve apoptosis suppression, increased proliferation, or HIV gag cross-reactivity. Instead, the findings suggest that intermittent or chronic expression of epitopes, such as DYS, drive inflation of activated CD4⁺ T cells that home to endothelial cells and have the potential to mediate cytotoxicity and vascular disease.

The Journal of Immunology, 2017, 199: 000–000.

Classical CD4⁺ and CD8⁺ memory T cell responses against viruses expand during primary infection and contract to low magnitudes during postinfection resolution (1). However, CD8⁺ T cell responses to select epitopes of human CMV (HCMV) (2, 3), rhesus CMV (4), and murine CMV (MCMV) (5–9) persist for decades at very high magnitudes after primary infection or during latency. This phenomenon is termed “memory inflation” and has been best characterized among CMV-specific CD8⁺ T cells that consist primarily of CD45RO⁺ CCR7⁻

CD27⁻ T cells (effector memory T cells [T_{EM}]) and their CD45RA⁺ revertants, CD45RO⁻ CCR7⁻ CD27⁻ T cells (effector memory-RA⁺ T cells [T_{EMRA}]) (8–12). CMV-specific CD8⁺ T cells express high levels of CX₃CR1 that bind CX₃CL1 (fractalkine), which is expressed on vascular endothelial cells (VECs), a major target of CMV latent infection (1).

Classical CMV-specific CD8⁺ T cells display an IL-7R α /CD127⁻, PD-1⁻ phenotype (capable of homeostatic proliferation controlled by IL-7 and other cytokines), whereas inflated

*Department of Pathology, Microbiology and Immunology, Vanderbilt University School of Medicine, Nashville, TN 37232; [†]Division of Infectious Diseases, Department of Medicine, Vanderbilt University Medical Center, Nashville, TN 37232; [‡]School of Human Sciences, University of Western Australia, Perth, Western Australia 6009, Australia; [§]Institute for Immunology and Infectious Diseases, Murdoch University, Murdoch, Western Australia 6150, Australia; [#]Stem Cell Transplantation, Division of Hematology/Oncology, Department of Medicine, Vanderbilt University Medical Center, Nashville, TN 37232; [¶]Peter Medawar Building for Pathogen Research, University of Oxford, Oxford OX1 3SY, United Kingdom; and ^{||}Department of Medicine, Laboratory Medicine, and Global Health, University of Washington, Seattle, WA 98195

¹S.A.K. and S.A.M. are cosenior authors.

ORCIDs: [0000-0003-0209-8470](#) (C.O.A.); [0000-0003-1318-8279](#) (M.A.P.); [0000-0001-6873-0198](#) (S.G.); [0000-0003-3859-2067](#) (W.J.M.); [0000-0002-7473-9129](#) (C.H.); [0000-0003-4307-9161](#) (P.K.); [0000-0003-1255-9023](#) (D.M.K.); [0000-0003-0098-7995](#) (S.A.K.); [0000-0002-7036-1309](#) (S.A.M.).

Received for publication June 13, 2017. Accepted for publication August 28, 2017.

This work was supported by National Institutes of Health (NIH) Grants P30 AI110527 (to S.A.M.), P01 AI030731 and R01 AI094019 (to D.M.K.), P50 GM115305 (to E.J.P.), T32 AI007474 (to S.A.K.), P01 AI030731 (to Lawrence Corey, principal investigator), UL1 TR000445 (to Gordon Bernard, principal investigator), HHSN272201300006C (to the NIH Tetramer Core Facility), and by National Institute of General Medical Sciences Grant T32 GM007347 (to C.O.A.).

C.O.A., M.A.P., S.G., C.W., P.K., E.J.P., D.M.K., S.A.K., and S.A.M. designed research studies; C.O.A., C.H., D.K.J., B.G.E., M.H.J., S.A.K., and S.A.M. acquired

samples; C.O.A., S.G., A.C., L.B., R.G., C.H., and D.K.J. conducted experiments; C.O.A., S.G., A.C., and L.B. acquired data; C.O.A., S.G., W.J.M., E.J.P., S.A.K., and S.A.M. analyzed data; C.O.A., M.A.P., P.K., D.M.K., S.A.K., and S.A.M. wrote the manuscript; and all authors edited the manuscript.

The TCR, TCR α , and TCR β CDR3 data presented in this article have been submitted to the National Center for Biotechnology Information Sequence Read Archive under accession number SRP113337 (<https://trace.ncbi.nlm.nih.gov/Traces/study/?acc=SRP113337&go=go>) and to the VDJdb database (<https://vdjdb.cdr3.net>).

Address correspondence and reprint requests to Dr. Simon A. Mallal, Vanderbilt University Medical Center, 1161 21st Avenue S, A-2200 MCN, Division of Infectious Diseases, Nashville, TN 37232. E-mail address: s.mallal@vanderbilt.edu

The online version of this article contains supplemental material.

Abbreviations used in this article: A2:NLV, A2:NLVPMVATV; ART, antiretroviral therapy; Bcl-2, B cell lymphoma-2; CI, confidence interval; ddPCR, droplet digital PCR; DR7⁺, DRB1*07:01; DR7:DYS, DR7-restricted DYS; DYS, DYSNTHSTRYV; EPD, EPDVYYTSQVFPTK; FRD, FRDYVDRFYKTLRAEQASQE; gB, glycoprotein B; HCMV, human CMV; IRB, Institutional Review Board; LCL, lymphoblastoid cell line; LIN, LINSTKIYSYFPVISVKVNQ; LN, lymph node; MCMV, murine CMV; MFI, median fluorescence intensity; pp65, phosphoprotein-65; PRS, PRSPTVFYNIPPMPLPPSQL; Q, glutamine; S, serine; T, threonine; TCR β , TCR β -joining; TCR β V, TCR β -variable; T_{EM}, effector memory T cell; T_{EMRA}, effector memory-RA⁺ T cell; TIGIT, T cell Ig and ITIM domain; tp1, time point 1; tp2, time point 2; TT, tetanus toxoid; VEC, vascular endothelial cell.

Copyright © 2017 by The American Association of Immunologists, Inc. 0022-1767/17/\$35.00

CMV-specific CD8⁺ T cells are CD127⁻, PD-1⁻, T cell Ig and ITIM domain (TIGIT)⁻, granzyme B⁺, and CX₃CR1⁺, with evidence suggesting that they are maintained by low-level exposure to persistent Ag from stochastic CMV reactivation (1, 13–16). These data suggest that inflated responses are maintained through recurrent stimulation by peptide-MHC (17–19) produced by persistent stochastic expression of specific CMV transcripts (20–22). These epitopes are presented to CMV-specific T cells by latent HCMV-infected nonhematopoietic reservoirs, including VECs, lymph node (LN) stroma cells, and cells in the bone marrow and lungs (1, 23–25). Maintenance of inflated CMV-specific T cell responses might also depend on their longer telomeres that positively correlate with persistence (26) or on epitope cleavage by constitutive proteasomes (6, 27).

CMV-specific CD4⁺ T cells suppress HCMV lytic replication (28) and maintain CD8⁺ T cell inflation (29). HCMV lysate-specific CD4⁺ T cells persist at high magnitudes in HIV⁺ HCMV⁺ coinfection (30), which might be due to higher HCMV disease burden (31, 32). Yet it is not known whether CD4⁺ T cells specific to individual HCMV epitopes undergo memory inflation in coinfected subjects. Glycoprotein B (gB) has the highest population prevalence of CD4 responses of any HCMV protein (33). gB polyprotein colocalizes to endosomes that process and present its class II epitopes directly from infected endothelial cells upon IFN- γ -induced HLA class II expression (28, 34, 35) without needing professional APCs. gB-loaded endosomes are also secreted as immunogenic exosomes that stimulate CD4⁺ memory T cells (36, 37). In DRB1*07:01 (DR7⁺) persons, the most immunogenic gB epitope is the extremely conserved DYSNTHSTRYV (DYS) epitope that is recognized by cytotoxic CX₃CR1⁺ CD4⁺ T cells (11, 38).

HIV⁺ HCMV⁺ coinfection is implicated in the emerging higher incidence of HCMV-related non-AIDS comorbidities of cardiovascular diseases, including hypertension, coronary artery disease, and stroke, despite suppressive antiretroviral therapy (ART) (31, 39–43). These disease risks are further increased in coinfecting subjects with elevated CD4⁺ T cell activation (CD38⁺ HLA-DR⁺) (44), which are mostly CMV-reactive (45) and are reduced by anti-CMV therapy (46). Indeed, CMV-reactive CD4⁺ CX₃CR1⁺ T cells have been proposed as potential mediators of these comorbidities (36, 47, 48). Increased magnitudes of CD4⁺ CX₃CR1⁺ T cells positively correlate with arterial stiffness (49), and these populations significantly decrease in magnitude after anti-CMV therapy (50). However, the specific epitopes and activation phenotype of these CMV-reactive CD4⁺ CX₃CR1⁺ T cells remain unknown.

We propose a model in which HIV⁺ HCMV⁺ coinfection increases stochastic nonproductive HCMV reactivation that drives CD4 memory inflation. We hypothesized that HLA-DR7-restricted DYS-specific (DYS⁺) CD4⁺ T cells from HIV⁺ HCMV⁺ DR7⁺ subjects undergo increased memory inflation compared with similar cells from HIV⁻ HCMV⁺ DR7⁺ subjects, and these cells upregulate CX₃CR1, CD38, and HLA-DR. To test this hypothesis, we studied the ex vivo frequencies among subjects, response magnitudes, and properties of DYS⁺ CD4⁺ T cells in HIV⁺ HCMV⁺ long-term nonprogressors (to avoid confounding effects of HIV-induced subclinical HCMV expression) and in HIV⁻ HCMV⁺ individuals using a DR7-restricted DYS (DR7:DYS) tetramer, because cytokine-based assays can underestimate actual T cell response magnitudes, and the expression of phenotypic markers can change after restimulation (51). The threshold for inflation was arbitrarily set at 1% of circulating CD4⁺ T cells, because there is no standard minimum in the literature.

Materials and Methods

Subjects

HIV⁺ and HIV⁻ subjects were randomly recruited through the Vanderbilt Comprehensive Care Clinic (Institutional Review Board [IRB] 030005), Vanderbilt Stem Cell Clinic (IRB 061215), and the Australian Red Cross (IRB 2011/02) after they signed consent forms authorized by the respective IRBs. HCMV⁺ or HCMV⁻ status was determined by CMV IgG serology. Class II HLA typing was performed at the Institute for Immunology and Infectious Diseases (Perth, WA) or at DCI Tissue Typing Laboratory (Nashville, TN). PBMCs were isolated, frozen, and thawed as previously described (52).

Tetramers and peptides

The National Institutes of Health Tetramer Core Facility (contract HHSN272201300006C) synthesized DRB1*07:01-restricted PE-, allophycocyanin-, and BV421-conjugated HCMV gB_{217–227} | DYS; HCMV phosphoprotein-65 (pp65)_{177–191} | EPDVYYTSASFVFPTK (EPD) (53); human CLIP_{87–101} | PVSKMRMATPLLMQA; tetanus toxoid (TT) precursor_{586–605} | LINSTKIYSYFPSPVISVKVNQ (LIN) (54); and HIV gag_{293–312} | FRDYVDRFYKTLRAEQASQE (FRD) (55) tetramers. DRB1*07:01: PRSPTVFYNIPPMLPPSQL (PRS) (EBV EBNA_{276–295}) tetramer was synthesized by Benaroya Research Institute (Seattle, WA) (56). A2:NLVPMVATV (A2:NLV; CMV pp65_{495–503}) tetramer was synthesized in the laboratory as described (57) using peptides manufactured by Schafer-N and reagents obtained from Dr. Søren Buus and ImmunAware. The National Institutes of Health AIDS Reagent Program (Division of AIDS, National Institute of Allergy and Infectious Diseases) provided HCMV pp65 Peptide Pool (overlapping 15-mers; catalog number 11549), HIV-1 PTE Gag Peptide Pool (overlapping 15-mers; catalog number 12437), and CMV AD169 strain (catalog number 1910). Lyophilized DYS, EPD, FRD, PRS, and LIN peptides and 19 overlapping high DR7-affinity HIV gag peptides from the HIV-1 PTE Gag Peptide Pool (predicted by NetMHCII 2.2 Server) were synthesized at ≥98% purity (GenScript).

Flow cytometry

Cryopreserved PBMCs were thawed, washed in PBS (Corning), and disentangled with Nuclease S7 (Roche). Depending on the assay, PBMCs were left untouched or were negatively enriched for CD4⁺ T cells (Miltenyi Biotech). Using our modified version of a class II tetramer stain protocol (56), we first stained for dead cells (Life Technologies) and washed with human Ab serum (Corning). Next, we stained with pretitrated tetramer volumes at 37°C (1 h), anti-CCR7 Ab at 37°C (20 min), and room temperature surface protein stain (20 min) and, if necessary, intracellular Ab stain (20 min) at room temperature after fixation and permeabilization (BD Biosciences). mAbs included CCR7-BV421 (clone 150503), CD3-BV711 (clone UCHT1), CD4-PeRCP-Cy5.5 (clone RPA-T4), CD45RO-PE-CF594 (clone UCHL1), CD27-PE-Cy7 (clone M-T271), CD14-V500 (clone M5E2), CD19-V500 (clone HIB19), IFN- γ -FITC (clone B27), TNF- α -PE-Cy7 (clone MA11), CD4-FITC (clone SK3), B cell lymphoma-2 (Bcl-2)-PE (clone Bcl-2/100), granzyme B-FITC (clone GB11), CX₃CR1-PE (clone 2A9-1), Ki-67-PE-Cy7 (clone B56), CD57-FITC (clone NK-1), CD45RA-PE-Cy7 (clone L48), CD38-PE-Cy7 (clone HIT2), and HLA-DR-FITC (clone G46-6) (all from BD Biosciences); CD8-allophycocyanin-AF750 (clone 3B5) (Invitrogen); PD-1-PE (clone EH12.2H7) (BioLegend); TIGIT-PE-Cy7 (clone MBSA43) and CD28-PE-Cy7 (clone CD28.2) (eBioscience); and custom CD127-PE-Cy5.5 (clone R34.34) (Beckman Coulter). Cells were sorted with a FACSAria IIIu or were collected on an LSR Fortessa (both from BD Biosciences). FlowJo (v10.1r5; TreeStar) was used for analysis. Only background-subtracted tetramer⁺ response magnitudes three times greater than the respective CLIP tetramer response magnitudes were considered positive. Median fluorescence intensity (MFI) analyses were done only on samples stained and collected the same day.

ELISPOT

IFN- γ ELISPOT was conducted on a Biomek FX^P high-throughput platform (Beckman Coulter) using the Human IFN- γ ELISpot^{BASIC} (HRP) kit (Mabtech). Cryopreserved PBMCs were thawed and rested overnight in R10 media (52) before triplicate stimulations of 150,000–250,000 cells per well in MultiScreen-IP Filter Plates (Millipore) with no peptide, or with 0.001 μ g/ μ l final concentrations of DYS, EPD, PRS, or LIN epitope or HCMV pp65 Peptide Pool, HIV-1 PTE Gag Peptide Pool, or anti-human CD3 (Mabtech). IFN- γ spot-forming units were developed using tetramethylbenzidine (Mabtech) and counted with an EliSpot Reader (Autoimmun Diagnostika) after drying. Positive spots = data > background mean + three times background SEM (38).

Bulk-cell TCR sequencing

TCR β gene sequencing of DNA extracted (catalog number DC6701; Promega) from bulk-sorted DYS $^+$ and DYS $^-$ CD4 $^+$ TEM or T_{EMRA} was completed and bioinformatically analyzed by Adaptive Biotechnologies. CDR3 proportions, productive template fractions, and clonalities and V(D)J segments were analyzed using immunoSEQ Analyzer v3.0. Circos plots were generated using VDJtools and circize (58, 59). The TCR CDR3 data have been submitted to the NCBI Sequence Read Archive under accession number SRP113337 (<https://trace.ncbi.nlm.nih.gov/Traces/study/?acc=SRP113337&go=go>).

TCR artificial expression and stimulation by LCL-pulsed epitopes

TCR α and TCR β CDR3 sequences of Subject 10027's DYS $^+$ sorted single cells were determined using a previously published technique (60). Briefly, single cells were sorted into separate wells in a 96-well plate containing RT-PCR buffer using a FACS Aria IIIu cell sorter (BD Biosciences) for three rounds of PCR amplification using nested, barcoded, TCR-specific, and Illumina Paired End primers (60). Purified PCR products were sequenced on an Illumina MiSeq System. After sequence analyses, TCR α and TCR β products with identical barcodes were selected for full TCR gene completion using the international ImMunoGeneTics database. Following published methods (61), the DYS-specific TCR α and TCR β genes were cloned into pSELECT-GFPzeo plasmids (InvivoGen) and expressed in Jurkat cells (clone E6-1, TIB-152; American Type Culture Collection) along with pNFAT-Luc (Affymetrix). These cells and lymphoblastoid cell lines (LCLs) were maintained in R10 media (52). DYS or control epitopes were pulsed with the LCLs to stimulate the DYS-specific TCRs expressed on the Jurkat cells. Luciferase absolute light units were measured using a FilterMax F5 Multi-Mode Microplate Reader (Molecular Devices). The TCR α and TCR β CDR3 data have been submitted to the NCBI Sequence Read Archive under accession number SRP113337 (<https://trace.ncbi.nlm.nih.gov/Traces/study/?acc=SRP113337&go=go>) and the VDJdb database (<https://vdjdb.cdr3.net>).

Droplet digital PCR

Droplet digital PCRs (ddPCRs) were performed entirely using a QX200 AutoDG Droplet Digital PCR System (Bio-Rad). For both assays, plates of droplets of PCR mixture were automatically generated with an AutoDG and TaqMan oil for probes, heat-sealed, and amplified with a C1000 Touch Thermal Cycler. Droplets were read using a Droplet Reader. The magnitude of false-positive responses in no-template controls was 15% (data not shown). DNA concentrations \pm 95% confidence interval (CI) were determined only from wells with $>12,000$ droplets using QuantaSoft v1.7.4.0917 after manually setting the positive droplet threshold above the negative droplet signal of the no-template controls in the same plate. Primer and probe concentrations were 900 and 250 nM, respectively. All PCRs were multiplexed with RPP30 housekeeping gene. For HCMV DNA quantitation, 20 μ l of PCR mixture was prepared using DNA, ddPCR SuperMix for Probes, water, and the following CMV primers and probes: IE1-specific forward primer 5'-TGAAGCGCCGCATTGA-3', IE2-specific reverse primer 5'-TG-GCCCGTAGGTCTACCCA-3', and IE1-specific probe 5'-6FAM-TCTGCAT-GAAGGTCTTGCCCAGTACATCC-TAMRA-3'. Thermocycling conditions were 50°C (2 min), 95°C (10 min), and 40 cycles of 95°C (15 s) with 60°C (1 min) (2°C/s ramp rate). For modified HIV DNA quantitation (62), 20 μ l of PCR mixture was prepared similarly, but using the following HIV LTR primers and probes instead: forward primer 5'-AGCACTCAAGGCAAGCTTA-3', reverse primer 5'-TGTACTGGGTCTCTGGTAG-3', and probe 5'-FAM-GCAGTGGGTCCTAGTTAGCCAGAGAG-3IABkFQ-3'. Thermocycling conditions were 95°C (10 min), 40 cycles of 94°C (30 s) with 60°C (1 min), and 98°C (10 min) (2°C/s ramp rate).

Statistics

GraphPad Prism v7.0a was used for nonparametric two-tailed analyses of the Wilcoxon matched-pairs signed rank test (paired), the Mann–Whitney U test (nonpaired), and the Spearman rank correlation (ρ) (linear regression).

Results

HLA-DR7-restricted DYS $^+$ CD4 $^+$ T cells are inflated in HIV $^+$ HCMV $^+$ DR7 $^+$ subjects compared with HIV $^-$ HCMV $^+$ DR7 $^+$ subjects

Following the gating hierarchy in Supplemental Fig. 1, we verified tetramer specificity using DR7:CLIP tetramer stain of CD4-enriched PBMCs from time point 1 (tp1; no ART) of eight

HIV $^+$ HCMV $^+$ DR7 $^+$ subjects (Fig. 1A, Table I). We also confirmed the HLA-DR7 restriction of the response by staining CD4-enriched PBMCs from seven coinfecting subjects lacking the HLA-DR7 allele (i.e., DR7 $^-$) (Supplemental Fig. 2A). To determine the HLA-DR7 $^+$ DYS $^+$ CD4 $^+$ T cell response magnitude in HIV $^+$ HCMV $^+$ DR7 $^+$ subjects, tp1 CD4-enriched or untouched PBMCs were stained with DR7:DYS tetramer. We detected high DYS $^+$ CD4 $^+$ T cell responses in seven subjects (0.43–17.91%), with six of them displaying inflated responses (Fig. 1A). To determine whether DYS $^+$ CD4 $^+$ T cell inflation was abrogated after ART-induced HIV suppression, we stained aviremic PBMCs from later time points (9.5-y median time lapse) of four coinfecting individuals (time point 2 [tp2], Table I) with the tetramer and detected values ranging from 0.11 to 26.34% (Fig. 1B). Inflation magnitude did not correlate with age (possibly due to the small sample size, which could be increased in future studies), HIV infection duration, nadir CD4 count, or HIV load (data not shown).

Importantly, we observed significantly lower magnitudes of DYS $^+$ CD4 $^+$ T cells (0.01–1.32%) in 10 HIV $^-$ HCMV $^+$ DR7 $^+$ subjects (Fig. 1C) compared with HIV $^+$ HCMV $^+$ DR7 $^+$ individuals (median 0.06% versus 4.76%, $p = 0.004$, Fig. 1D). Samples from tp1 of Subject 10013 and tp2 of Subjects 10004, 10027, and 10032 were used in this and all future experiments, unless otherwise indicated. CD4 counts of the HIV $^-$ cohort were unavailable for absolute DYS $^+$ CD4 count comparisons. To confirm that these cells are undergoing memory inflation, we analyzed DYS $^+$ CD4 $^+$ T cells from five time points of two HIV $^+$ DR7 $^+$ subjects spanning a period of up to 12 y and detected stable magnitudes and absolute counts (Fig. 1E, 1F, respectively). Together, these findings identify inflated CD4 $^+$ T cells against HLA-DR7-restricted DYS epitope of HCMV gB in HIV $^+$ HCMV $^+$ coinfecting subjects.

HLA-DR7-restricted CD4 $^+$ T cell responses to other persistent and nonpersistent epitopes are low in HIV $^+$ HCMV $^+$ DR7 $^+$ subjects

Tetramer stains of CD4 $^+$ T cells specific for a DR7-restricted highly conserved HCMV pp65 EPD epitope, which were absent in HIV $^+$ HCMV $^+$ DR7 $^-$ subjects (Supplemental Fig. 2B), revealed significantly lower magnitude ranges in the HIV $^+$ HCMV $^+$ DR7 $^+$ cohort (0.01–1.87%, Supplemental Fig. 2C) compared with inflated DYS $^+$ CD4 $^+$ T cells in this cohort (median 0.04% versus 4.76%, $p = 0.02$, Fig. 1D). We did not detect any memory inflation of these EPD $^+$ CD4 $^+$ T cells in four longitudinal samples obtained from the two subjects with the highest DYS-specific inflation over a ≤ 12 -y period (Fig. 1E, 1F). A similar trend was observed in the HIV $^-$ HCMV $^+$ DR7 $^+$ cohort between EPD $^+$ (0.003–0.04%, Supplemental Fig. 2D) and DYS $^+$ CD4 $^+$ T cells (median 0.001% versus 0.06%, $p = 0.03$, Fig. 1D). As observed for DYS $^+$ CD4 $^+$ T cells, EPD $^+$ CD4 response magnitudes were also significantly higher in the HIV $^+$ HCMV $^+$ DR7 $^+$ cohort than in the HIV $^-$ HCMV $^+$ DR7 $^+$ cohort ($p = 0.002$, Fig. 1D), confirming a recent report using pp65 peptide pools instead (63). To determine whether the inflation could be due to generalized HIV-induced inflammation, we compared the magnitudes of CD4 $^+$ T cells specific for DR7-restricted TT, EBV, or HIV epitopes from the HIV $^+$ DR7 $^+$ subjects with their DYS $^+$ CD4 $^+$ T cell counterparts. We observed that the magnitudes of responses to these other epitopes were undetectable or very low compared with the inflated DYS-specific response ($p = 0.0078$ for each comparison, Supplemental Fig. 2E). To evaluate potential CD8 $^+$ T cell inflation, we stained PBMCs from Subject 10027, who has the highest DYS $^+$ CD4 inflation (26.34%) and carries an HLA-A2:01 allele with A2:NLV tetramer, but detected an NLV-specific CD8 $^+$ T cell response magnitude of only 0.75% (Supplemental Fig. 2F). Collectively, these results indicate that other DR7 $^+$ epitope-

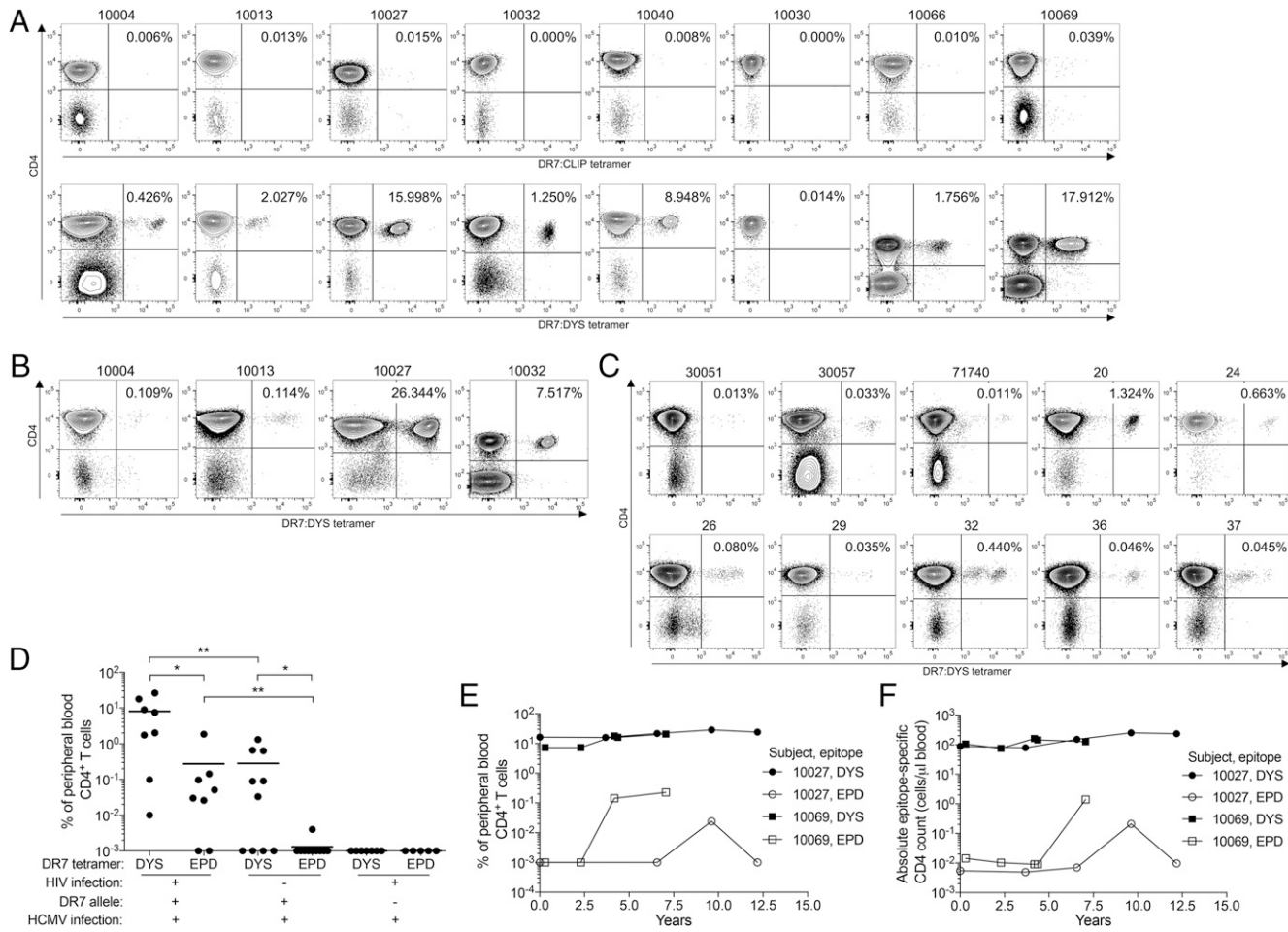


FIGURE 1. HLA-DR7-restricted HCMV gB DYS epitope specific CD4⁺ T cells undergo memory inflation in HIV⁺ DR7⁺ subjects. CD4-enriched or untouched PBMCs from HIV⁺ DR7⁺ subjects were stained with DR7:CLIP or DR7:DYS tetramer for their tp1 samples (no ART) (*n* = 8) (**A**) and tp2 samples (on ART) (*n* = 4) (**B**). (**C**) DR7:DYS tetramer staining of HIV⁻ DR7⁺ subjects' PBMCs (*n* = 10). (**D**) Response magnitude comparisons of DYS⁺ and EPD⁺ CD4⁺ T cells from HIV⁺ HCMV⁺ DR7⁺ (*n* = 8; tp1 of Subject 10013 and tp2 of Subjects 10004, 10027, and 10032), HIV⁻ HCMV⁺ DR7⁺ (*n* = 10), and HIV⁺ HCMV⁺ DR7⁻ (*n* = 5–7) subjects determined simultaneously from the same samples per subject. Values represent at least three biological replicates with means, with the exception of the HIV⁺ HCMV⁺ DR7⁻ cohort (no replicates). Longitudinal response magnitudes (**E**) and absolute counts (**F**) of DYS⁺ and EPD⁺ CD4⁺ T cells from Subjects 10027 and 10069. **p* ≤ 0.05, ***p* ≤ 0.01.

specific CD4⁺ T cells in most coinfecting subjects are present at lower magnitudes than DYS⁺ CD4⁺ T cells.

DYS⁺ CD4⁺ T cells consist of T_{EM} and/or T_{EMRA} subsets

We determined the memory phenotype of DYS⁺ CD4⁺ T cells by measuring surface expression of memory markers CD45RO, CCR7, and CD27 to define T_{EM}, T_{EMRA}, central (CD45RO⁺ CCR7⁺ CD27⁺),

transitional (CD45RO⁺ CCR7⁻ CD27⁺), naive (CD45RO⁻ CCR7⁺ CD27⁺), and intermediate (CD45RO⁻ CCR7⁻ CD27⁺) subsets (Supplemental Fig. 1) (10). Compared with the non-DYS⁺ (DYS⁻) CD4⁺ T cells, DYS⁺ CD4⁺ T cells from HIV⁺ HCMV⁺ DR7⁺ subjects were biased toward T_{EM} (46.6–97.97% versus 6.1–51.9%, *p* = 0.016) and T_{EMRA} (0.03–48.1% versus 0.4–16.7%, *p* = 0.078) (Fig. 2A), and similar observations were made in the HIV⁻ HCMV⁺

Table I. Characteristics of HIV⁺ HCMV⁺ DR7⁺ subjects

| Subject ID | HLA-DRB1 Alleles | Time Point | Age (y) | HIV Infection (y) | CD4 T Cell Count/ μ l Blood | HIV Load (RNA Copies/ml Plasma) | Time on ART (y) |
|------------|------------------|------------|---------|-------------------|---------------------------------|---------------------------------|-----------------|
| 10004 | 07:01, 03:01 | 1 | 58 | 22 | 203 | <50 | — |
| | | 2 | 62 | 26 | 181 | <50 | 2.17 |
| 10013 | 07:01, 04:08 | 1 | 47 | 22 | 420 | 5354 | — |
| | | 2 | 60 | 35 | 380 | <50 | 5.0 |
| 10027 | 07:01, 03:01 | 1 | 66 | 14 | 378 | 7340 | — |
| | | 2 | 75 | 23 | 977 | <50 | 7.17 |
| 10032 | 07:01, 03:01 | 1 | 46 | 5 | 543 | 2837 | — |
| | | 2 | 56 | 15 | 886 | <50 | 4.42 |
| 10040 | 07:01, 13:01 | 1 | 47 | 14 | 1161 | <50 | — |
| 10030 | 07:01, 09:01 | 1 | 60 | 13 | 856 | <50 | — |
| 10066 | 07:01, 07:01 | 1 | 52 | 14 | 1063 | <50 | — |
| 10069 | 07:01, 08:04 | 1 | 46 | 6 | 903 | 2470 | — |

The dashes indicate no data.

DR7⁺ cohort (Fig. 2B). Most CD45RO⁻ DYS⁺ and DYS⁻ CD4⁺ T cells were CD45RA⁺, as shown in Subject 10027 (Fig. 2C).

DYS-stimulated CD4⁺ T cells secrete IFN- γ and TNF- α

Most HIV⁺ HCMV⁺ DR7⁺ PBMC samples stimulated with DYS produced IFN- γ in high-throughput ELISPOT, and only Subject 10013 responded to EPD (Fig. 2D), indicating that tetramer staining was more sensitive or that the cells were dysfunctional. Subject 10004 did not respond to either epitope on the IFN- γ ELISPOT, possibly as the result of dysfunction or anergy. One of three screened HIV⁻ HCMV⁺ DR7⁺ subjects responded to DYS stimulation (Fig. 2E). Responses to HIV FRD epitope, EBV PRS epitope, or TT LIN epitope were relatively diminished in HIV⁺ DR7⁺ subjects compared with DYS-induced responses and were not detected in HIV⁻ DR7⁺ subjects (Fig. 2D, 2E, respectively). Dual IFN- γ and TNF- α intracellular cytokine staining of Subject 10027's PBMCs, which produced the largest IFN- γ ELISPOT response to DYS, confirmed that the ELISPOT responses originated from CD4 cells, and not CD8 cells, and suggested that these inflated cells were likely polyfunctional (Fig. 2F), as previously reported (11, 35).

Inflated DR7⁺ DYS⁺ CD4⁺ T cells have highly restricted TCR β repertoires

TCR analyses were conducted only on subjects with adequate DYS⁺ CD4 magnitudes of response for bulk cell sorting and sequencing: HIV⁺ Subjects 10027, 10040, 10069, and 10032 (26.34, 8.95, 17.91, and 7.52%, respectively) and HIV⁻ Subject 20 (1.32%) as a control. We observed highly restricted TCR β -variable (TCR β V) and TCR β -joining (TCR β J) gene pairing in bulk-sorted T_{EM} and T_{EMRA} subsets of DYS⁺ CD4⁺ T cells compared with the more diverse DYS⁻ counterparts in all subjects (Fig. 3).

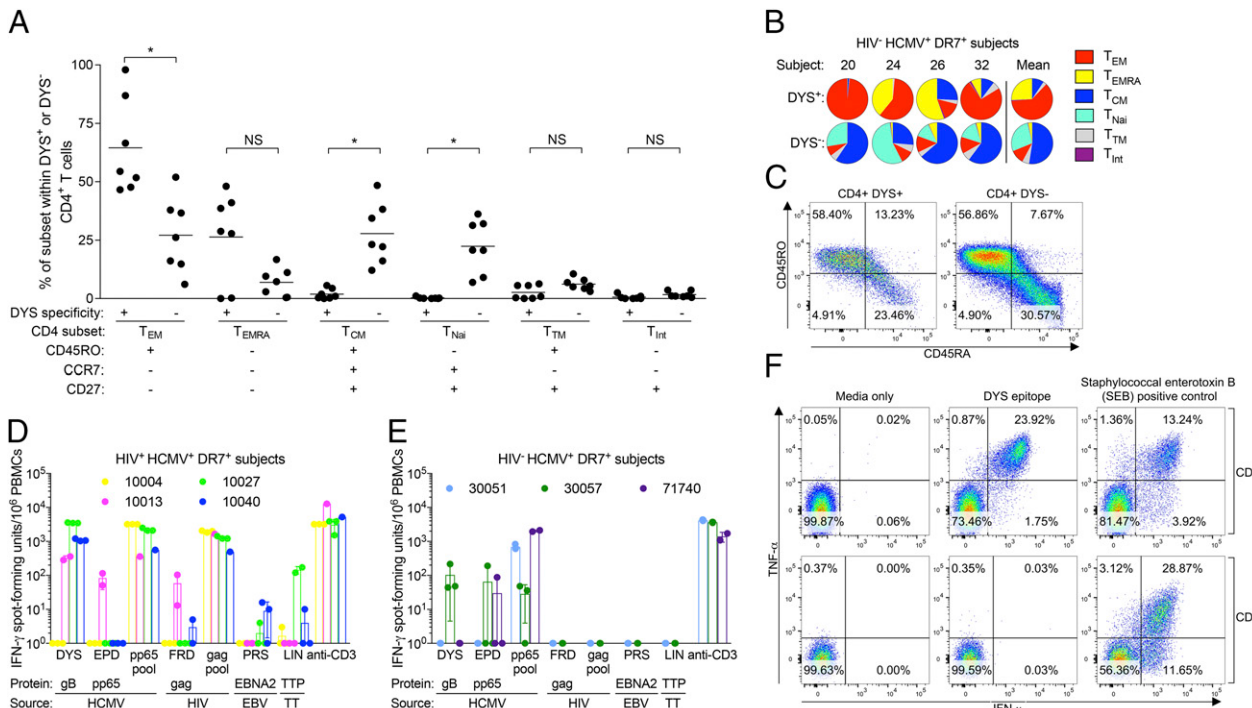


FIGURE 2. CD4⁺ T cells specific for the DYS epitope consist of T_{EM} and T_{EMRA} subsets and secrete cytokines upon DYS stimulation. **(A)** Response magnitude comparisons of DYS⁺ and DYS⁻ CD4⁺ T cell subsets from HIV⁺ HCMV⁺ DR7⁺ subjects ($n = 7$). PBMCs were stained with the tetramer and memory markers to identify the subsets. Plots show grand means and represent at least two biological replicates. **(B)** Normalized magnitudes of CD4 subsets within DYS⁺ or DYS⁻ CD4⁺ T cells from HIV⁻ HCMV⁺ DR7⁺ subjects with sufficient tetramer⁺ response for analyses. **(C)** CD45RO and CD45RA staining of Subject 10027's PBMCs. Background-corrected IFN- γ ELISPOT responses of PBMCs from HIV⁺ HCMV⁺ DR7⁺ ($n = 4$; tp1) **(D)** and HIV⁻ HCMV⁺ DR7⁺ ($n = 3$) **(E)** subjects upon stimulation with 0.001 μ g/ml DYS, EPD, FRD, PRS, or LIN epitopes and the following controls: HCMV pp65 overlapping 15-mer peptide pool, HIV's gag overlapping 15-mer peptide pool, and anti-human CD3. Data represent technical triplicates except in conditions without mean \pm SD. **(F)** Intracellular cytokine staining of Subject 10027's PBMCs after DYS or SEB stimulation. * $p \leq 0.05$.

The dominant TCR β V and TCR β J gene families of each individual's DYS⁺ CD4⁺ T cells made up 69.5–99.7% of the DYS⁺ CD4⁺ T cell repertoire and were identical between their T_{EM} and T_{EMRA} subsets (Supplemental Fig. 3). However, the dominant TCR β V and TCR β J gene families of DYS⁻ CD4⁺ T cells were lower (10.42–56.46%) and different between T_{EM} and T_{EMRA} subsets (Supplemental Fig. 3). These findings indicate a strong TCR β conservation among inflated DYS⁺ CD4⁺ T cells.

Inflated DR7⁺ DYS⁺ CD4⁺ T cells use nearly monoclonal CDR3s

We analyzed the CDR3 repertoires of productive V(D)J rearrangements (in-frame and without stop codons) of the bulk-sorted DYS⁺ CD4⁺ T cells and observed that they were dominated by specific clones with unique V(D)J rearrangements (69.41–99.64%, median = 91.37%) (Fig. 4). Interestingly, we discovered that 97.29 and 7.6% of the productive DYS⁺ CD4⁺ T_{EM} CDR3 repertoires of Subject 20 (HIV⁻) and Subject 10069 (HIV⁺), respectively, were identical. T_{EM} CDR3 analysis of an HIV⁻ HCMV⁻ subject showed no clonal expansion (data not shown), suggesting that clonal expansion among DYS⁻ T_{EM} CDR3s might be tied to HCMV⁺ status. The DYS⁺ and DYS⁻ CDR3 clonal dominance reflected their respective TCR β gene family distributions. DYS⁺ T_{EM} and T_{EMRA} dominant clones within each subject were identical, and this is likely a reflection of the reversible T cell differentiation from T_{EM} (CD45RO⁺ CD45RA⁻) to T_{EMRA} (CD45RO⁻ CD45RA⁺) (11).

In vivo stimulation of inflated cells involves NFAT-mediated cellular activation and proliferation upon TCR ligation by peptide-MHC. To confirm this activity and the accuracy of the clonal CDR3 sequence, we simulated the Ag-presentation conditions for Subject 10027 using autologous B cell-derived LCLs and the DYS epitope to

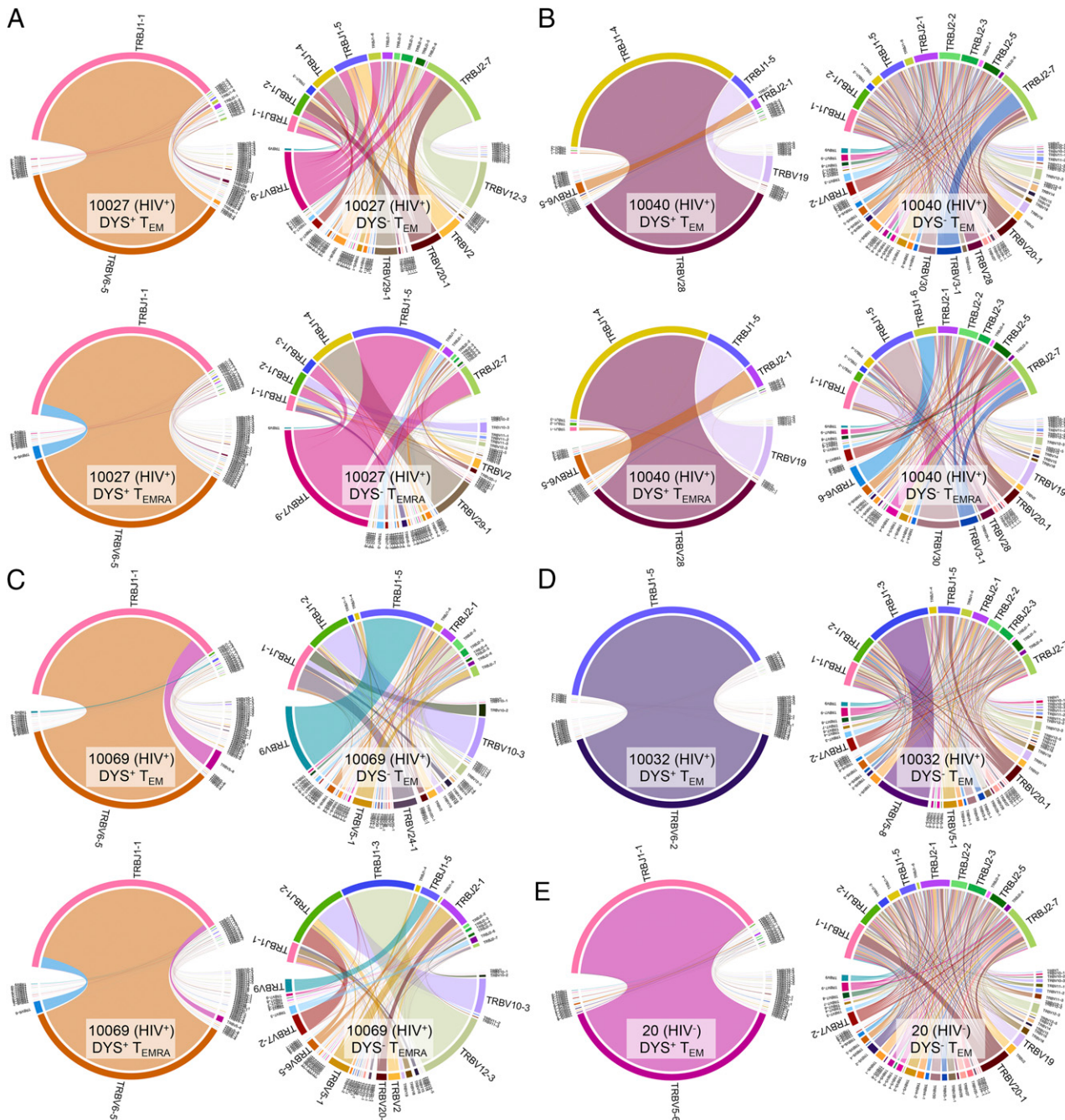


FIGURE 3. Productive TCR β V and J gene pairs of bulk-sorted inflated DYS $^+$ CD4 $^+$ T cells are highly restricted. TCR β V and TCR β J gene family pairings of T $_{EM}$ and/or T $_{EMRA}$ subsets of productive DYS $^+$ and DYS $^-$ CD4 TCRs from Subject 10027 (**A**), Subject 10040 (**B**), Subject 10069 (**C**), Subject 10032 (**D**), and Subject 20 (**E**). Data shown represent single experiments. V and J gene pairs are connected by stems between their arcs. Arc lengths reflect gene family proportions within the sample's repertoire. High-magnitude V and J gene families are emphasized.

stimulate autologous DYS $^+$ $\alpha:\beta$ TCR expressed on Jurkat cells with an NFAT-mediated luciferase reporter. Using single-cell sorting and TCR sequencing, we first determined the paired $\alpha:\beta$ TCR CDR3 sequences of autologous DYS $^+$ CD4 $^+$ T cells to be TCR α CAGRSSNTGKLIF CDR3 (TCR α V25 and TCR α J37) and TCR β CASIHQGSTEAFF CDR3 (TCR β V6-5 and TCR β J1-1) that matched Subject 10027's nearly monoclonal CDR3 sequence (Fig. 5A). After TCR expression and stimulation with autologous DYS-pulsed DR7 $^+$ LCLs, we detected a dose-dependent luciferase luminescence that was not present with no epitope, a different epitope (EPD), or a DR7 $^-$ LCL (Fig. 5A). Subject 10069's LCL (DR7, DR8) confirmed that DYS was presented by DR7 and not DR3, which was the other DRB1 allele of Subject 10027 (Fig. 5A).

Clonality comparison revealed that DYS $^+$ CD4 $^+$ T $_{EM}$ and T $_{EMRA}$ were significantly more clonal compared with DYS $^-$ counterparts and were almost monoclonal in Subject 10032 ($p = 0.0078$, Fig. 5B). We verified the expectation of more productive V(D)J rearrangements within DYS $^+$ CD4 $^+$ T cells compared with DYS $^-$ CD4 $^+$ T cells, because the former were sorted based on specific HLA-restricted epitope recognition ($p = 0.0078$, Fig. 5C). These results suggest that DYS $^+$ CD4 $^+$ T cells are inflated via a highly clonal mechanism that likely involves DYS stimulation.

Different DYS $^+$ CDR3 clones share conserved amino acids

We assessed whether potential amino acid conservation among the different dominant DYS $^+$ CDR3s of all subjects could explain their

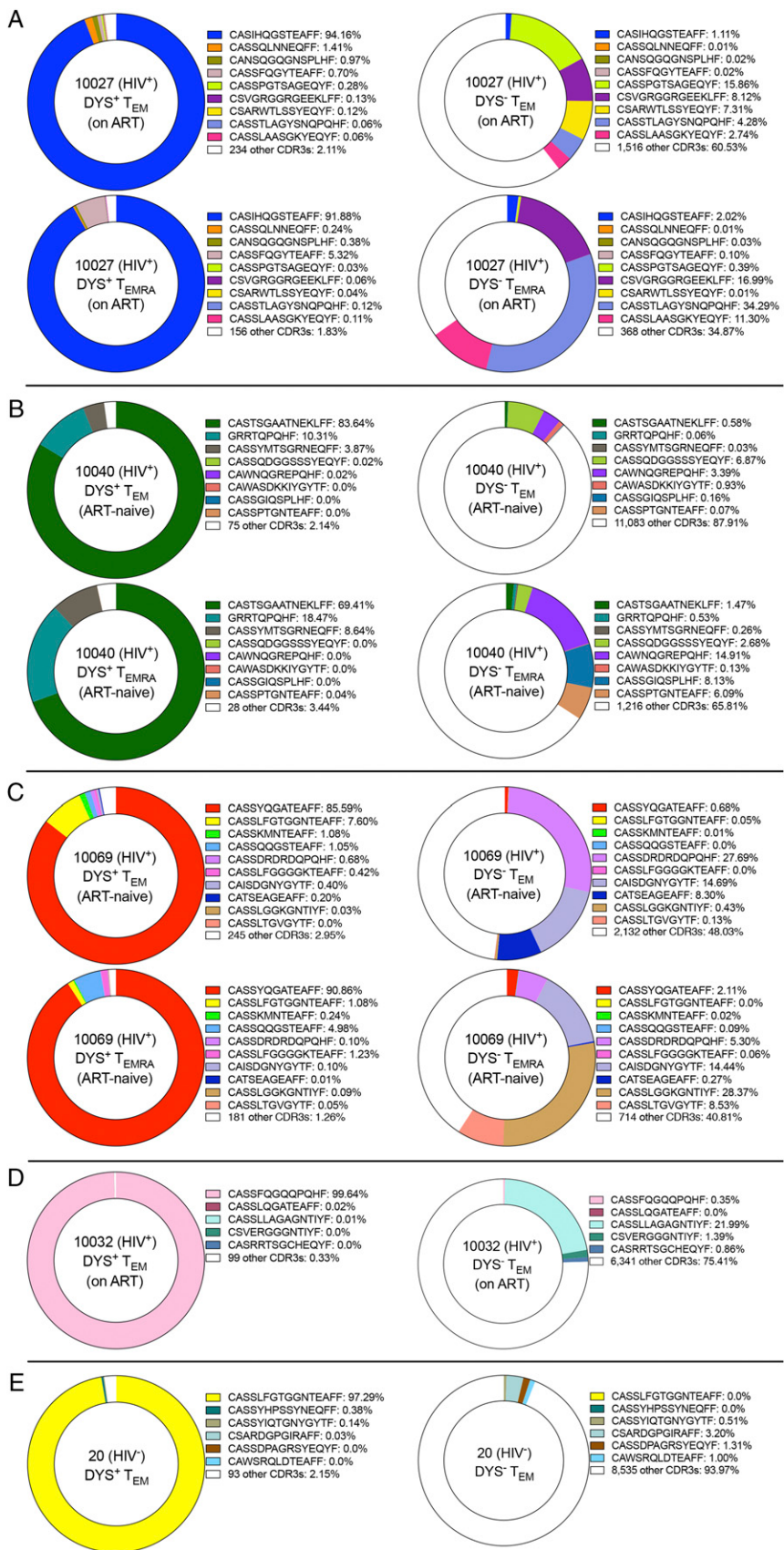


FIGURE 4. Inflated DYS⁺ CD4⁺ T cells have nearly monoclonal productive CDR3s. Productive and unique TCR β CDR3 clones of DYS⁺ and DYS⁻ TEM and/or TEMRA subsets from Subject 10027 (A), Subject 10040 (B), Subject 10069 (C), Subject 10032 (D), and Subject 20 (E). Data represent single experiments.

Inflated DR7⁺ DYS⁺ CD4⁺ T cells are CD127⁻ TIGIT⁻ granzyme B⁺

We measured plasma HCMV DNA load of all subjects but detected no viral DNA despite being HCMV⁺, suggesting that inflation of these circulating cells was not due to ongoing HCMV replication in the blood. Other samples, such as saliva and semen, in which active HCMV replication has been reported, were unavailable for testing. We next determined whether inflated CD4⁺ T cells displayed the similar CD127⁻ PD-1⁻ TIGIT⁻ granzyme B⁺ phenotype of inflated CMV-specific CD8⁺ T cells (1, 14, 16). For all onward comparison experiments of inflated DYS⁺ CD4⁺ T cells ($n = 7$), we used HIV⁻ HCMV⁻ controls ($n = 10$) to provide contrast with classical T_{EM} and avoid other potential inflammatory HCMV epitope-specific responses, as well as because HIV⁺ HCMV⁻ subjects are extremely rare. We focused on only T_{EM} because DYS⁺ T_{EMRA} were present in only five HIV⁺ HCMV⁺ DR7⁺ subjects. We compared CD127, PD-1, and TIGIT expression on DYS⁺ CD4⁺ T_{EM} with CD4⁺ T_{EM} from HIV⁻ HCMV⁻ controls and detected significantly lower CD127 ($p = 0.025$), no difference in PD-1 ($p = 0.364$), and significantly lower TIGIT ($p = 0.0001$) among the inflated cells (Fig. 6A–C). The dual IFN- γ and TNF- α secretion in Fig. 2F also suggests that these cells are not exhausted. To further determine polyfunctionality, we compared ex vivo intracellular granzyme B levels of DYS⁺ CD4⁺ T_{EM} from HIV⁺ HCMV⁺ DR7⁺ subjects with controls and detected significantly higher levels on cells with DYS specificity ($p = 0.0001$, Fig. 6D), confirming previous cytotoxicity (11, 28, 35, 38, 64) and polyfunctionality (11, 35) reports for DYS⁺ CD4⁺ T cells. Bcl-2 protein MFIs of inflated DYS⁺ CD4⁺ T cells were not different compared with controls ($p = 0.536$, Fig. 6E). None of these protein levels correlated with the magnitude of DYS⁺ CD4 inflation (data not shown). These findings reveal that inflated DYS⁺ CD4⁺ T cells are CD127⁻ PD-1⁻ TIGIT⁻ granzyme B⁺.

Inflated DR7⁺ DYS⁺ CD4⁺ T cells are CX₃CR1^{high} and are not undergoing higher proliferation

Latent HCMV reservoirs present endogenous DYS epitopes to DYS⁺ CD4⁺ T cells (28, 35, 65). Therefore, we hypothesized that such reservoirs expand with HIV coinfection to cause memory inflation. Although we could not directly measure HCMV reservoir size, we further hypothesized that expanded HCMV latent reservoirs, including VECs, would express more CX₃CL1 and, consequently, correlate with higher expression of CX₃CR1 on inflated DYS⁺ CD4⁺ T cells. Indeed, these cells had significantly

higher CX₃CR1 MFI compared with controls ($p = 0.0007$, Fig. 7A), confirming previous reports (11). To determine whether effective TCR stimulation by DYS-presenting latent reservoirs caused ongoing proliferation in vivo and, by extension, memory inflation, we measured ex vivo Ki-67⁺ levels within inflated DYS⁺ CD4 T_{EM} and detected a slightly wider range of, but not significantly higher, magnitudes compared with controls ($p = 0.474$, Fig. 7B), in keeping with studies on MCMV epitope-specific CD8⁺ T cell inflation (5, 9). Using CD57 and CD28 dual staining of Subject 10027's tp2 PBMCs, we observed that <2% of CD4⁺ DYS⁺ T cells displayed the CD57⁺ CD28^{-/-} phenotype for replicative senescence (Fig. 7C) (66). CX₃CR1 and Ki-67 levels did not correlate with DYS⁺ CD4 inflation magnitudes (data not shown). These findings suggest that inflated DYS⁺ CD4 T cells might interact with HCMV reservoirs that express CX₃CL1, and their inflation is not linked to increased ongoing proliferation.

Inflation is not caused by DR7-restricted HIV gag epitope cross-reactivity

TCR cross-reactivity is ubiquitous and can occur between unrelated pathogens, including HIV (gag) and influenza A virus (67). To assess cross-reactive TCRs' role in inflation, we repeated the HLA-epitope-TCR simulation experiment using 19 high-affinity DR7-restricted HIV gag epitopes instead, but detected no response (Fig. 7D). Also, HIV viremia was not associated with a significant increase in inflation compared with aviremia ($p = 0.625$, Fig. 7E). These findings suggest that the inflation is not likely caused by cross-reactive HIV gag epitopes.

We also investigated whether HCMV might latently infect the inflated CMV-specific memory CD4⁺ T cells that it induces. We optimized ddPCR quantitation of HCMV DNA using HCMV AD169 strain but did not detect any HCMV DNA in DYS⁺ CD4⁺ T cells (Supplemental Fig. 4A, 4B).

Inflated DYS⁺ CD4⁺ T cells display elevated levels of CD38 or HLA-DR but less often coexpress CD38 and HLA-DR

We measured CD38 and HLA-DR dual and individual expression on inflated DYS⁺ CD4⁺ T cells. Although we observed no significant difference in their CD38⁺ HLA-DR⁺ coexpression magnitude compared with HIV⁻ HCMV⁻ DYS⁻ T_{EM} controls ($p = 0.091$, Fig. 8A), we observed significantly higher levels of CD38⁺ HLA-DR⁺ coexpression on their DYS⁻ T_{EM} counterparts within the HIV⁺ HCMV⁺ cohort compared with the same controls ($p = 0.0001$, Fig. 8A). Additionally, individual protein analyses

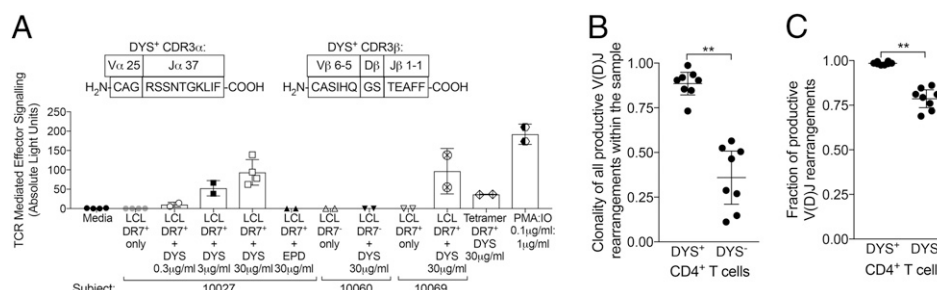


FIGURE 5. Expressed clonal TCR of inflated DYS⁺ CD4⁺ T cells recognize the DR7-restricted DYS epitope. **(A)** Subject 10027's DYS⁺ single-cell α : β TCR CDR3 sequences and NFAT-mediated luciferase luminescence response of DR7⁺ LCL-presented serially diluted DYS epitope stimulation of DYS⁺ TCR. Subject 10027's DYS⁺ α : β TCR gene sequences were determined from single-cell sorting and expressed using plasmids in an NFAT-luciferase reporter Jurkat cell line for stimulation. Graph shows mean \pm SD. Conditions with two data points represent technical replicates, whereas those with four represent two biological replicates of two technical replicates. **(B)** Clonality comparison of productive CDR3s of DYS⁺ with DYS⁻ CD4⁺ T_{EM} and T_{EMRA} subsets from Subjects 10027, 10040, 10069, 10032, and 20. Clonality fractions were bioinformatically determined after productive entropy normalization. Values near 1 reflect more clonal. **(C)** Fractional comparison of productive V(D)J rearrangements of DYS⁺ to DYS⁻ CD4⁺ T_{EM} and T_{EMRA} subsets from all five subjects. Values near 1 reflect fewer out-of-frame sequences or stop codons. Data in (B) and (C) represent single experiments for each subject with mean \pm 95% CI. ** $p \leq 0.01$.

Table II. Dominant CDR3 β s of inflated DYS $^+$ CD4 $^+$ T cells share conserved polar, neutral amino acids

| Subject ID | CDR3 Frequency (%) | TCRβV Family | | | | V Segment (start of CDR3) | | | | N1 | | D Segment | | N2 | | J Segment | | TCRβ Family | |
|------------|--------------------|--------------|-----|-----|-----|---------------------------|-----|------------|-----|-----|-----|-----------|-----|-----|-----|-----------|--|-------------|-----|
| | | C | A | S | I | H | Q | G | S | T | E | A | F | F | 1-1 | | | | |
| 10027 | 94 | 6-5 | tgt | gcc | agc | atc | cat | <u>caa</u> | S | egg | agc | A | act | ttc | ttt | | | | |
| 10040 | 84 | 28 | C | A | S | T | | | G | ggg | A | A | N | gaa | | | | | 1-4 |
| 10069 | 91 | 6-5 | tgt | gcc | agc | act | | | tcg | gca | gca | A | aat | L | F | F | | | 1-1 |
| 10032 | 99 | 6-2 | C | A | S | Y | | | Q | G | A | T | E | aaa | cgt | ttt | | | 1-5 |
| 20 | 96 | 5-6 | tgt | gcc | agc | agt | tat | F | egg | ggc | ggc | act | gaa | P | H | F | | | 1-1 |
| | | | C | A | S | S | | | Q | G | Q | T | | Q | | | | | |
| | | | tgt | gcc | agc | agt | | | caa | ggg | cag | | | ccc | cag | cat | | | |
| | | | C | A | S | S | L | F | G | G | N | T | E | A | F | F | | | |
| | | | tgt | gcc | agc | agg | tgg | tcc | ggg | aca | ggg | aac | act | gaa | gtt | ttt | | | |

Conserved Q, S, and T within the D segment are underlined. The dominant CDR3s were identical for DYS⁺ CD4⁺ T_{EM} and T_{TEMRA} subsets in all subjects.

revealed significantly higher levels of CD38 and HLA-DR ($p = 0.03$, $p = 0.03$, Fig. 8B, 8C, respectively). There was a stepwise increase in the mean expression from DYS⁻ T_{EM} of HIV⁻ HCMV⁻ to DYS⁻ T_{EM} of HIV⁻ HCMV⁺ to DYS⁻ and DYS⁺ T_{EM} of HIV⁺ HCMV⁺ subjects. These protein levels on DYS⁺ CD4⁺ T cells did not correlate with the magnitudes of DYS⁺ CD4 inflation (data not shown). CD38 was elevated on naive T cells, as expected (68). Finally, we quantified the latent HIV DNA in Subject 10027's DYS⁺ CD4⁺ T cells but did not detect any enrichment without or with ART compared with the DYS⁻ counterparts, despite the inflation ($p = 0.25$, $p = 0.031$, respectively, Supplemental Fig. 4C). HIV was not detected in enriched EPD⁺ CD4⁺ T cells, but low cell numbers might have limited the sensitivity. Overall, these findings indicate that inflated DYS⁺ CD4⁺ T cells do contribute to the increased T cell activation associated with the higher risk for HCMV-related non-AIDS comorbidities in HIV⁺ HCMV⁺ subjects, but further studies are required to define the specific subsets of activated cells that correlate most closely with these adverse outcomes.

Discussion

In this article, we show memory inflation of HLA-DR7-restricted HCMV epitope-specific CD4⁺ T cells in HCMV⁺ long-term nonprogressor HIV subjects that could potentially contribute to the higher T cell activation associated with elevated risks for HCMV-related non-AIDS cardiovascular comorbidities in such coinfecting patients. Ex vivo DR7:DYS tetramer stains revealed persistent inflated percentages of HCMV DYS⁺ CD4⁺ T cells in our HIV⁺ HCMV⁺ DR7⁺ subjects that consisted primarily of T_{EM} and T_{EMRA} subsets, and secreted IFN-γ and TNF-α upon in vitro DYS stimulation of their nearly monoclonal TCR repertoires. The 28.8% DYS⁺ CD4 response magnitude of Subject 10027 measured in time point 4 of the longitudinal analyses is the largest reported CD4 response magnitude against DYS epitope to our knowledge and is similar to the 24% magnitude of a DQ6-restricted pp65₄₁₋₅₅ LLQTG_iHVRVSQPSL-specific CD4 response (11), although the HIV status of the subject was not specified. It is not clear why Subject 10030 had an extremely low DYS⁺ CD4⁺ T cell magnitude. We doubt that this was due to CMV sequence variation because the DYS epitope and adjacent residues involved in proteosomal cleavage are known to be completely conserved.

To our knowledge, our findings represent the first ex vivo and tetramer-based evidence for CD4 memory inflation in HIV⁺ subjects, and it is striking in frequency and magnitude for the DYS epitope. It is quite remarkable that DR7⁺ CD4 responses to other HCMV, TT, EBV, or HIV epitopes analyzed in the same cohort were significantly lower. The reduced magnitude of IFN- γ responses to stimulations by these additional epitopes was reflected in the lower absolute counts among the stimulated cells in the intracellular cytokine staining assay. Therefore, we believe that the inflation of DYS-specific CD4⁺ T cells is more likely due to specific HLA–epitope–TCR interactions and is unlikely to be due to HIV-induced inflammation. This is also supported by the finding of a highly enriched CDR3 clonotype in HIV⁻ Subject 20. Also, it does not appear that this is an intrinsic feature of persistent viruses, because EBV epitope-specific responses were of low magnitude or absent within the same individuals. Although we were unable to measure these responses among the HIV⁻ DR7⁺ cohort because of IRB restrictions on reinviting the subjects, we believe that their magnitudes will be similarly low or undetectable. The EPD⁺ CD4⁺ T cell response was of unusually high magnitude in HIV⁺ Subject 10013 at tp1 (1.87%) and tp2 (1.4%, data not shown). This individual was also the only subject in

Table III. Dominant CDR3 β s of DYS $^-$ CD4 $^+$ T cells do not share conserved polar, neutral amino acids

Q within the D segment is underlined.

whom secreted IFN- γ was detected upon EPD stimulation. These findings suggest that the EPD epitope may drive a memory-inflated response in HIV, and we cannot exclude the possibility that EPD might rarely drive a memory-inflated response in HIV $^-$ individuals. Interestingly, low-level DYS $^+$ CD4 $^+$ T cell responses were detected in all HIV $^-$ HCMV $^+$ DR7 $^+$ subjects, with the exception of one subject with 1.32% magnitude of response. The observation that one HIV $^-$ subject had DYS $^+$ CD4 $^+$ T cell inflation, which was predominantly of the T_{EM} phenotype, illustrates that memory inflation with this epitope can occur in HIV $^-$ subjects. However, the prevalence and magnitude of memory inflation were substantially higher with HIV coinfection. Taken together, the findings suggest that CD4 $^+$ memory inflation can occur in HIV $^-$ individuals, but HIV acts to increase the prevalence and magnitude.

It is not fully understood how CMV, and why only CMV, induces chronic memory inflation and why this property has been conserved in mice (5–9), rhesus macaques (4), and man (2, 3). The inflated DYS and comparatively lower EPD responses in five HIV coinfected subjects parallel recent reports of different epitopes from the same protein inducing both high- and low-magnitude responses (5, 8). Potential explanations for DYS-specific inflation include the translation of gB mRNA without HCMV replication (69), gB colocalization to endosomes and endogenous presentation (28, 35), and the secretion of such gB epitope-loaded endosomes as immunogenic exosomes (36, 37). Endogenous epitope processing and presentation have been demonstrated recently to drive CD8 memory inflation (6, 27). However, the low pp65 EPD-specific responses might be due to pp65 polyprotein absence in immunogenic exosomes (37). Yet, this mechanism does not explain the published DQ6-restricted pp65_{41–55} LLQTGIVRVSQPSL epitope-induced inflation (11), suggesting that multiple factors underlie inflation. Differential gene expression patterns (70) and the presence of higher-avidity TCRs specific for DYS might also play some role. It is important to note that cytotoxic CD4⁺ T cells, in general, are elevated in HIV infection (71). This may be due to low CCR5 expression, especially by CMV-specific CD4⁺ T cells, which protects such cells from HIV infection and might explain the lack of HIV DNA enrichment in our results (72).

Few studies have described the TCR repertoire of HLA class II-restricted epitope-specific CD4 responses based on tetramer-sorted cells, and most were conducted in vitro or without TCR sequencing (55, 73–83). Notably, some of the repertoires of these single epitope-specific T cells are diverse, with over six unique dominant TCR gene families (55, 73, 80, 83). Therefore, to our knowledge, our work represents the first combination of ex vivo, class II tetramer-derived, and deep sequencing-based identification of a nearly monoclonal TCR repertoire of inflated HLA-restricted epitope-specific CD4⁺ T cells at the resolution of the CDR3. We discovered three new DYS-specific TCR β V gene families, TCR β V6-2, TCR β V5-6, and TCR β V28, in addition to the published TCR β V6-5 (64). CDR3 sequencing confirmed that the inflations were driven by nearly monoclonal expansions, especially in Subject 10032, in whom 99.4% of all DYS⁺ TEM were a single clone. HIV[−] Subject 20's DYS⁺ CD4⁺ T cell clonality indicates that clonal expansion to DYS was not unique to HIV⁺ subjects, a finding that again suggests that HIV coinfection is not necessary for, but rather increases the likelihood of, and amplifies DYS⁺ CD4⁺ T cell inflation. To determine whether the inflation was unique to DYS, a comparison between bulk DYS⁺ CDR3s and those of EPD, LIN, PRS, or FRD epitope would have been sufficient; however, magnitudes of cells specific to these additional epitopes were too low for that analysis. CDR3 sequences within DYS[−] CD4 samples were generally polyclonal

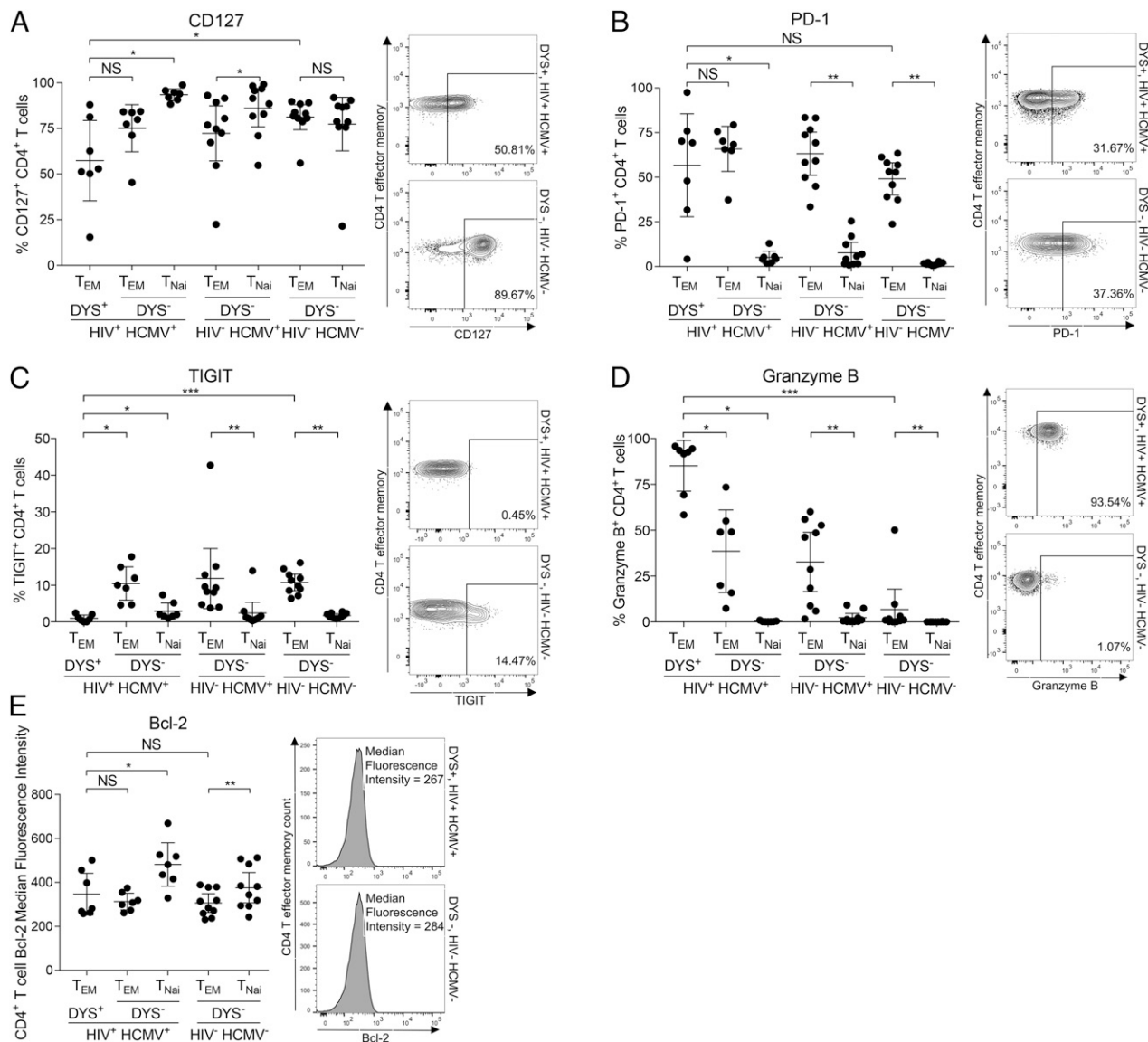


FIGURE 6. Inflated DYS⁺ CD4⁺ T cells have a CD127⁻ TIGIT⁻ granzyme B⁺ phenotype. Ex vivo comparisons of CD127 (**A**), PD-1 (**B**), TIGIT (**C**), or granzyme B (**D**) expression or Bcl-2 MFI (**E**) of DYS⁺ CD4⁺ T_{EM} of HIV⁺ HCMV⁺ subjects with DYS⁻ CD4⁺ T_{EM} of HIV⁻ HCMV⁻ controls. PBMCs were stained with tetramer and mAbs for surface PD-1, CD127, and TIGIT or for intracellular granzyme B and Bcl-2 proteins. HIV⁺ HCMV⁺, n = 7; HIV⁻ HCMV⁺, n = 10; and HIV⁻ HCMV⁻, n = 10. Graphs represent single experiments for each subject, with mean \pm 95% CI for all subjects. *p \leq 0.05, **p \leq 0.01, ***p \leq 0.001.

with a few exceptions. These noteworthy exceptions (Fig. 4, right column) might be driven by clonal expansions induced by epitopes that overlap with DYS, as observed in HCMV IE1 epitopes (84), or by other inflation-inducing epitopes of HCMV or other pathogens. The presence of the dominant DYS⁺ CDR3s within the DYS⁻ repertoire at relatively lower magnitudes reflected potential loss of tetramer binding, whereas the reverse could reflect non-specific binding to the DYS tetramer. The in vitro HLA-DR7-presented DYS stimulation of the inflated DYS⁺ CD4 TCR in our Jurkat cell-transfection system confirmed the specificity of the tetramer stain and accuracy of our bulk-cell and single-cell TCR α and TCR β sequencing. We analyzed the dominant DYS⁺ CDR3 sequences from different subjects for amino acid conservation because there are no reports of such conservation within inflationary CD4⁺ T cell CDR3s and even dominant clones of well-characterized noninflated HLA-A2:NLV CD8 responses from different individuals do not always contain conserved motifs (85). In addition to the published Q (64), we also discovered novel

conservations of S and T that preceded the germline glycine within the D segment of the different dominant DYS⁺ CD4 CDR3 clones. These amino acids are polar with neutral side chains that might serve as TCR binding residue sites for hydrogen bond formation with DYS and HLA-DR7. Further verification by crystallographic reconstruction of the DR7-DYS-TCR complex is required.

Inflation may be due to intermittent subclinical CMV reactivation or expression of specific transcripts. We detected no HCMV DNA in plasma samples from this cohort. Future studies could investigate this reactivation through monitoring of other specimens (e.g., saliva, semen). Although we were unable to determine the exact mechanism by which HCMV stimulates inflated responses in our human subjects, we analyzed ex vivo protein expression of DYS⁺ CD4⁺ T cells and observed similarities (CD127⁻ PD-1^{+/−} TIGIT⁻ granzyme B⁺) with those on inflated CMV-specific CD8⁺ T cells reported to be maintained by low-level exposure to Ags from stochastic HCMV reactivation (1,

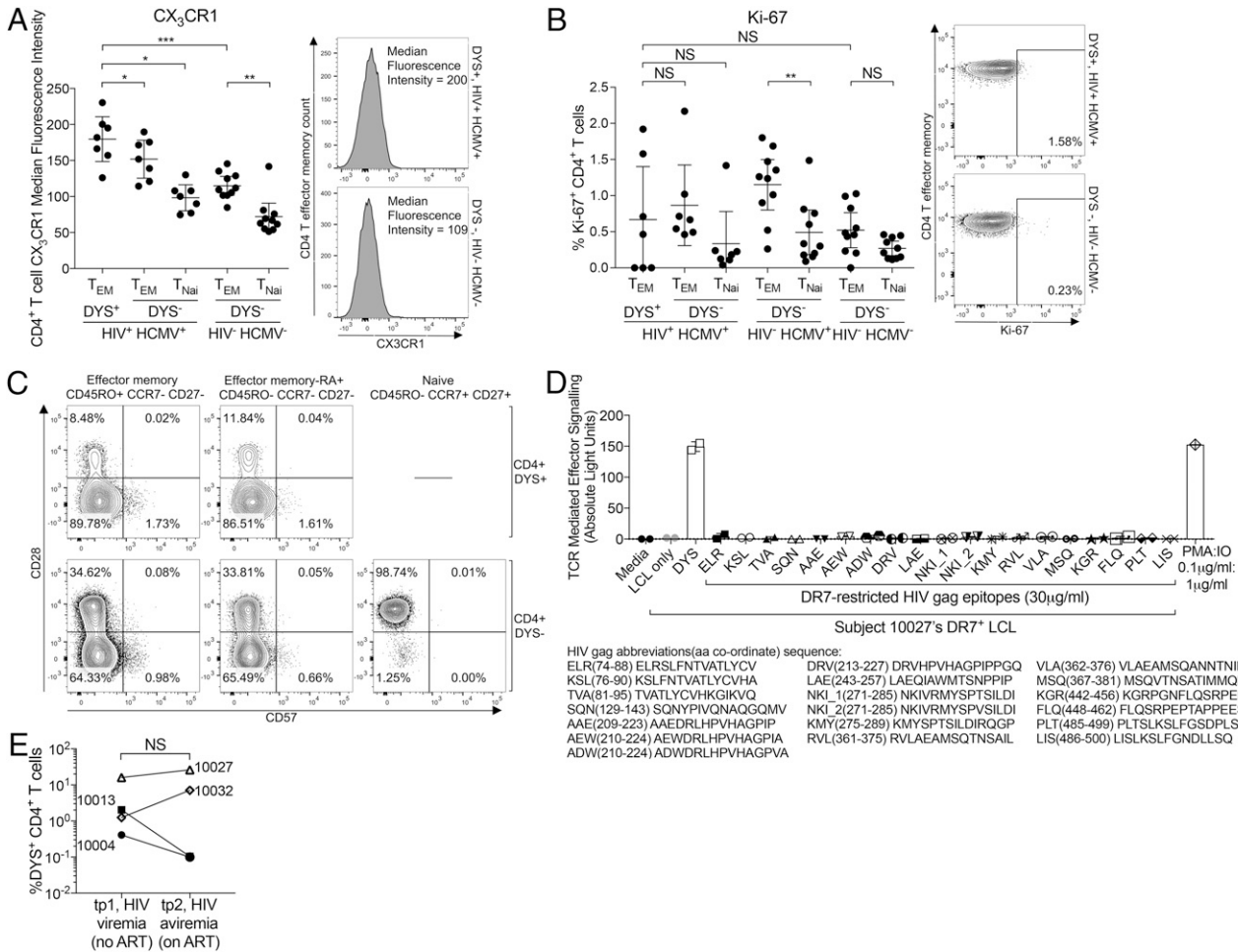


FIGURE 7. Inflated DYS⁺ CD4 T cells are CX₃CR1^{high}, not replicatively senescent, and do not cross-react with HIV gag proteins. Ex vivo comparisons of CX₃CR1 MFI (A) and Ki-67 response magnitude (B) of DYS⁺ CD4⁺ T_{EM} of HIV⁺ HCMV⁺ subjects with DYS⁻ CD4⁺ T_{EM} of HIV⁻ HCMV⁻ controls. HIV⁺ HCMV⁺, n = 7; HIV⁻ HCMV⁺, n = 10; HIV⁻ HCMV⁻, n = 10. (C) CD57 and CD28 expression of Subject 10027's DYS⁺ and DYS⁻ CD4⁺ T cells. (D) Luciferase luminescence response of 19 DR7-presented HIV gag epitopes' stimulation of Subject 10027's DYS⁺ TCR expressed in the Jurkat cell line. Data are mean ± SD of technical duplicates. (E) DYS⁺ CD4 magnitude change from tp1 (HIV viremia) to tp2 (HIV aviremia). Graphs in (A), (B), and (E) show mean ± 95% CI for all subjects and represent single experiments with no replicates, with the exception of (E), which shows technical replicates. *p ≤ 0.05, **p ≤ 0.01, ***p ≤ 0.001.

11, 16, 35). PD-1 might not be an appropriate coinhibitory protein to evaluate on DYS⁺ CD4⁺ T cells because of their low levels of CD28 (64), which has been recently shown to mediate PD-1 suppression of T cells (86, 87). The normal expression levels of antiapoptotic Bcl-2 suggest that DYS⁺ CD4⁺ T cell inflation is not due to apoptosis suppression but might be due to other maintenance mechanisms, such as longer telomeres (26), which could offset the normal rate of apoptosis. The persistence of inflated DYS⁺ T_{EM} and T_{EMRA} subsets, despite the lack of CCR7⁺ DYS⁺ T cell thymic emigrants, is explained by reports that thymectomy does not affect memory T cell inflation or homeostasis (88).

Surprisingly, Ki-67 data suggest that the DYS⁺ CD4⁺ T cell inflations were not driven to significantly higher proliferation. Although this observation might be due to cross-sectional sampling limitations, it does confirm findings in chronic MCMV models of inflation (5, 9). CD28 and CD57 analyses confirm that only a very limited number of the inflated cells are too senescent to replicate (66). The cause of inflation does not appear to involve DYS⁺ CD4⁺ TCR cross-reactivity with the DR7⁺ HIV gag epitopes either. But cross-reactivity with other DR7⁺ HIV epitopes cannot be excluded. We observed increased inflation in two subjects when HIV replication was suppressed to undetectable levels

with ART, suggesting that HIV replication is not required for maintenance of inflation.

The sites of HCMV latency are important (1), and HIV could alter the environment to help HCMV persist in long-lived non-hematopoietic cells in HCMV reservoir sites, such as LNs and VECs. VECs can serve as latent HCMV reservoirs and also express the CX₃CR1 ligand fractalkine. Vascular homing might bring CX₃CR1^{high} DYS⁺ CD4⁺ T cells in close contact with these potential HCMV reservoirs, resulting in restimulation and inflation. Although we did not detect HCMV DNA in the inflated cells, it is possible that they passively disseminate HCMV from LNs to vascular endothelium without getting infected, as LN-resident dendritic cells do for HIV. Herpes viruses, such as CMV, are species specific and cause life-long infection. Therefore, it is also possible that the inflated responses provide a degree of protective immunity against other infections, making them mutually beneficial to CMV and its host.

Although CD38⁺ HLA-DR⁺ coexpression on the inflated cells was not significantly elevated compared with HIV⁻ HCMV⁻ DYS⁻ T_{EM} controls, a wider distribution was observed with inflation. Remarkably, a similar comparison of CD38⁺ HLA-DR⁺ coexpression on the DYS⁻ T_{EM} counterpart of the inflated cells with the same controls revealed a significant difference. These

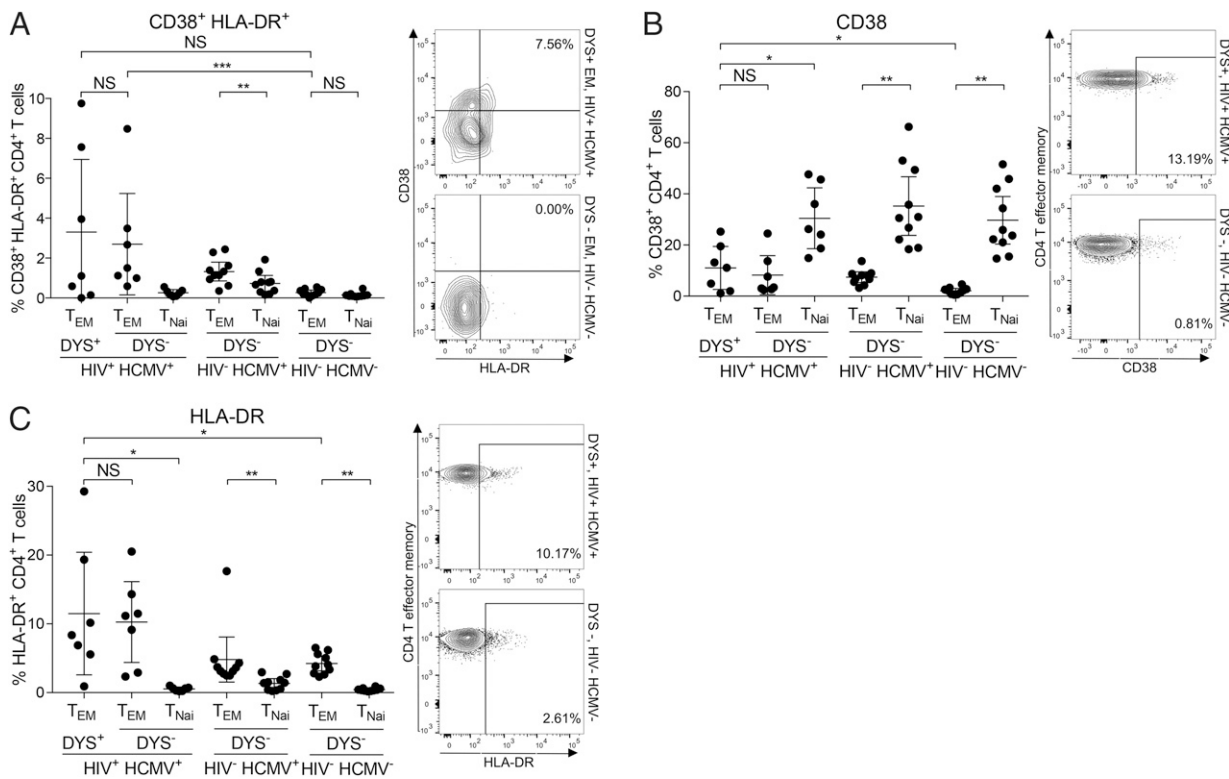


FIGURE 8. Inflated DYS⁺ CD4⁺ T cells have a wide distribution of CD38⁺ HLA-DR⁺ coexpression. Ex vivo comparisons of CD38⁺ HLA-DR⁺ (**A**), CD38⁺ (**B**), and HLA-DR (**C**) magnitudes on DYS⁺ CD4⁺ T_{EM} of HIV⁺ HCMV⁺ subjects with DYS⁻ CD4⁺ T_{EM} of HIV⁻ HCMV⁻ controls. HIV⁺ HCMV⁺, n = 7; HIV⁻ HCMV⁺, n = 10; HIV⁻ HCMV⁻, n = 10. Graphs represent single experiments for each subject and mean \pm 95% CI for all subjects. *p \leq 0.05, **p \leq 0.01, ***p \leq 0.001.

DYS⁻ T_{EM} consist of clonal CDR3 expansions (Fig. 4) that are potentially induced by other inflationary epitopes. Consequently, it is plausible that analyses of CD4 responses against a collection of inflationary epitopes or in a larger number of subjects might yield a difference. Neither statistical trend is due to generalized HIV-induced activation, because other pathogen/Ag-specific CD4⁺ T cells, including TT, are not necessarily more activated with HIV infection (45). This observation implies that inflated CD4⁺ T cells in these subjects could potentially contribute to the increased T cell activation associated with greater risks for HCMV-related non-AIDS cardiovascular comorbidities that continue to plague HIV⁺ subjects despite effective ART. The capacity of DYS⁺ CD4⁺ T cells to secrete granzyme B, IFN- γ , and TNF- α might facilitate the development of these comorbidities (36, 47, 48). A larger cohort of HIV⁺ HCMV⁺ DR7⁺ subjects with varying magnitudes of DYS⁺ CD4⁺ T cells is needed to directly evaluate the correlation of their activation with disease outcomes. The stepwise increments in CD38⁺ HLA-DR⁺ levels indicate that HCMV infection without HIV coinfection increases CD4⁺ T_{EM} activation in general, and HIV coinfection further synergizes such activation. This elevated activation might be tied to an HIV-induced latent HCMV reservoir expansion, presenting potential unintended negative consequences for HCMV vaccine candidates that possess inflation-inducing epitopes for all individuals, especially HIV⁺ DR7⁺ subjects. Although we studied HIV long-term nonprogressors, a previous study found that CMV lysate induces high levels of CMV-specific CD4⁺ T cells in HIV⁺ subjects with ART-induced HIV aviremia (30), suggesting that our findings may be applicable to a broader range of HIV-infected patients.

In conclusion, we have shown that HIV⁺ HCMV⁺ coinfection boosts CD4 responses to HCMV gB's DYS and pp65's EPD epi-

topes, resulting in primarily memory-inflated DYS⁺ CD4⁺ T cells. To our knowledge, this is the first ex vivo evidence of CD4⁺ T cell memory inflation against the DYS epitope in HIV⁺ subjects and nearly monoclonal CDR3 repertoire of inflated CD4⁺ T cells that contain novel conserved motifs. Although the underlying mechanism may be multifactorial, we hypothesize that increased low-level exposure and subsequent clonal expansion targeting the DYS epitope from stochastic HCMV reactivation or expression largely contribute to our observation. Our findings suggest that memory inflation-inducing epitopes might contribute to the immunopathogenesis of non-AIDS comorbidities and raise safety implications for CMV vaccines that contain inflation-inducing epitopes that should be considered in trials being planned in HIV-infected and non-HIV-infected subjects. This work also suggests that the relative contributions of conventional and inflated CMV-specific T cell responses to protection of the host from infection or malignancy, vaccine responsiveness, or comorbidities of aging, such as vascular disease, should be considered separately.

Acknowledgments

We are very grateful to all donors who participated in this study. We thank the Vanderbilt-Ingram Cancer Center for HIV⁻ samples, and the Vanderbilt Flow Cytometry Core for data acquisition. In no particular order, we also thank Mark Watson, Ian James, Søren Buus, Rita Smith, David Haas, Heather Long, John Koethe, Alec Redwood, Kaija Strautins, Kristina Williams, Katie White, Wannakuwatte Fernando, Katherine Konvinse, and Jessica Thomas for donor recruitment, blood draws, and helpful discussions.

Disclosures

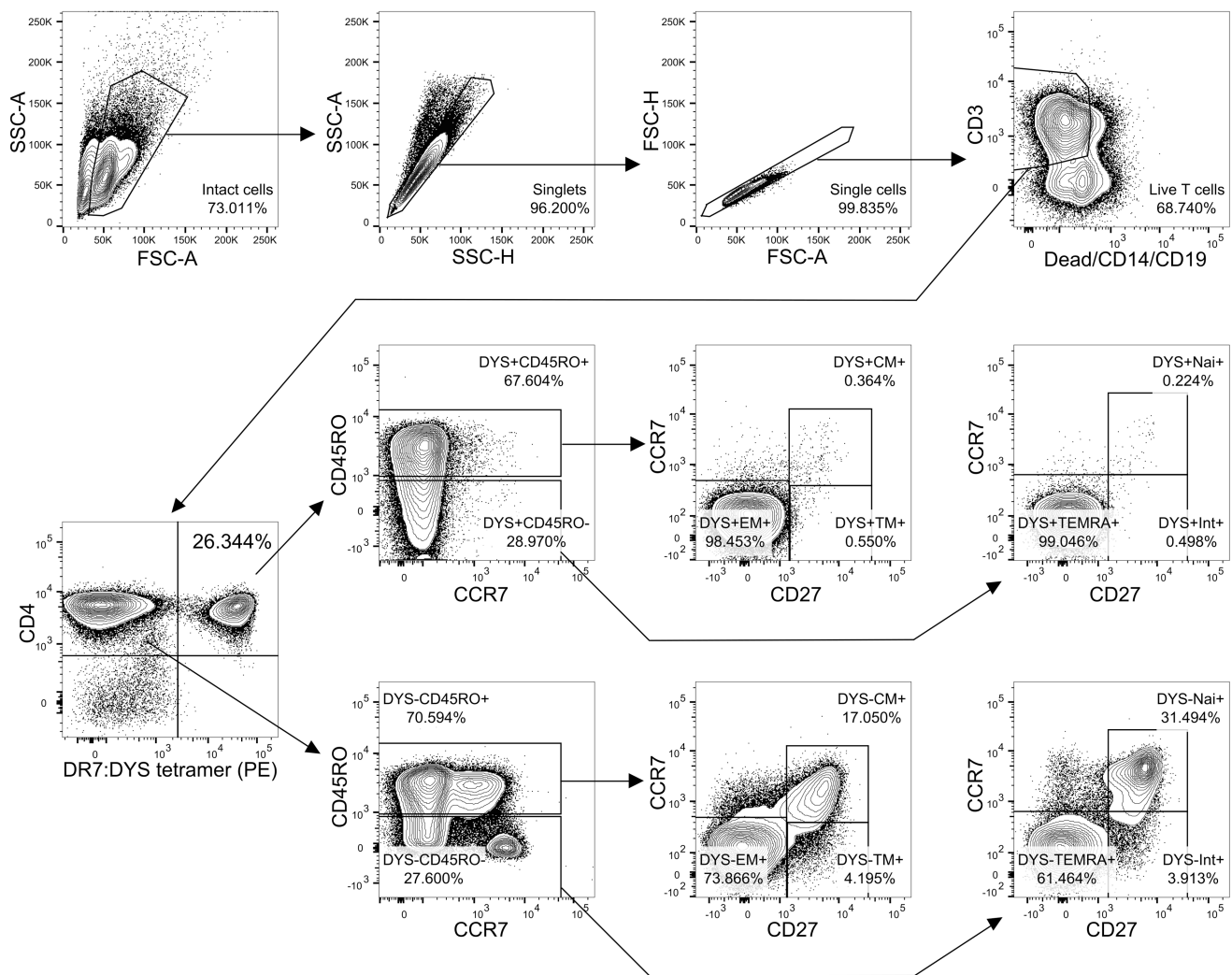
The authors have no financial conflicts of interest.

References

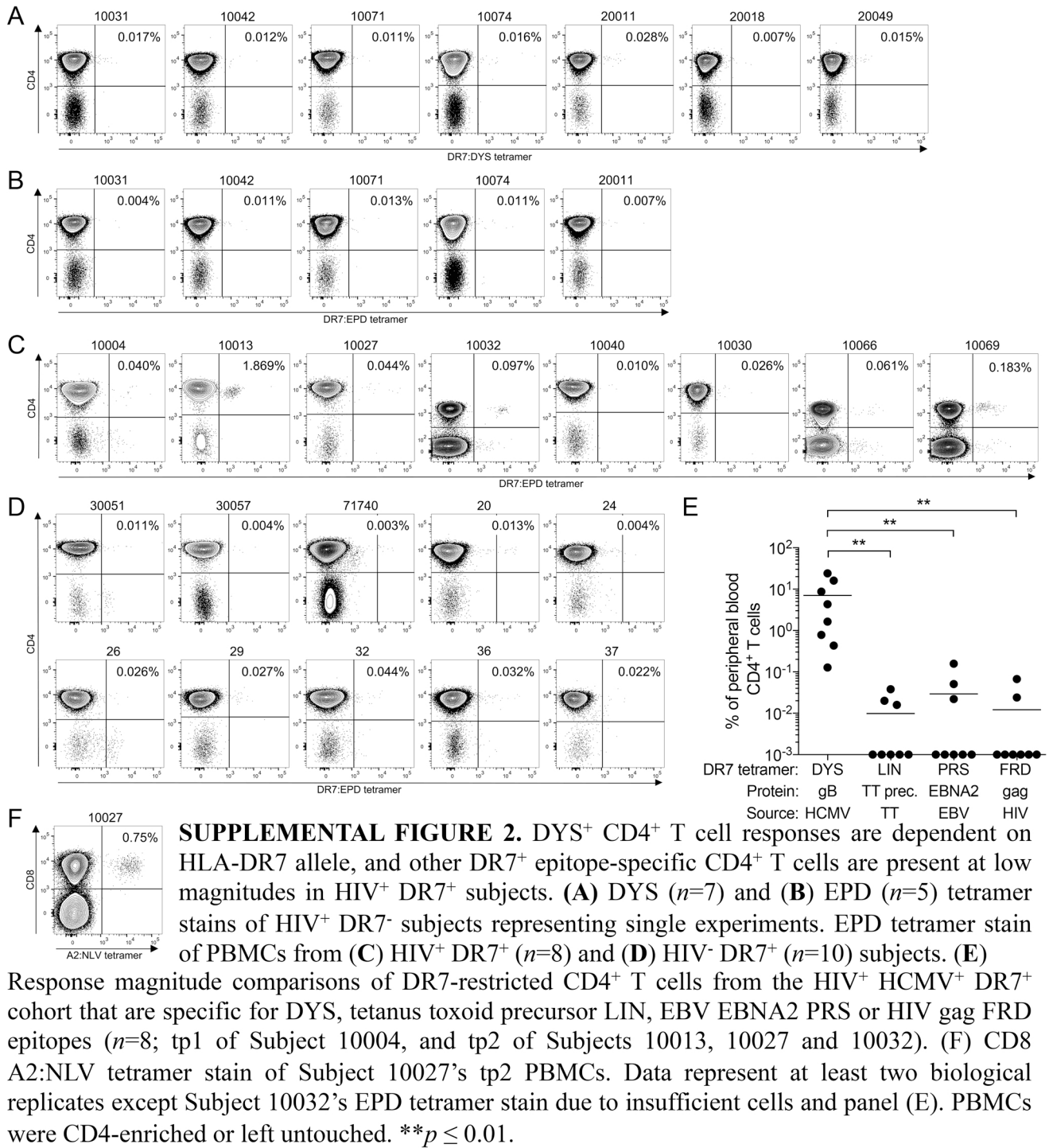
1. Klennerman, P., and A. Oxenius. 2016. T cell responses to cytomegalovirus. *Nat. Rev. Immunol.* 16: 367–377.
2. Waller, E. C., E. Day, J. G. Sissons, and M. R. Wills. 2008. Dynamics of T cell memory in human cytomegalovirus infection. *Med. Microbiol. Immunol.* 197: 83–96.
3. Klarenbeek, P. L., E. B. Remmerswaal, I. J. ten Berge, M. E. Doorenspleet, B. D. van Schaik, R. E. Eseldt, S. D. Koch, A. ten Brinke, A. H. van Kampen, F. J. Bemelman, et al. 2012. Deep sequencing of antiviral T-cell responses to HCMV and EBV in humans reveals a stable repertoire that is maintained for many years. *PLoS Pathog.* 8: e1002889.
4. Cicin-Sain, L., A. W. Sylvester, S. I. Hagen, D. C. Siess, N. Currier, A. W. Legasse, M. B. Fischer, C. W. Koudelka, M. K. Axthelm, J. Nikolich-Zugich, and L. J. Picker. 2011. Cytomegalovirus-specific T cell immunity is maintained in immunosenescent rhesus macaques. *J. Immunol.* 187: 1722–1732.
5. Bolinger, B., S. Sims, L. Swadling, G. O'Hara, C. de Lara, D. Baban, N. Saghal, L. N. Lee, E. Marchi, M. Davis, et al. 2015. Adenoviral vector vaccination induces a conserved program of CD8(+) T cell memory differentiation in mouse and man. *Cell Reports* 13: 1578–1588.
6. Dekhtarenko, I., R. B. Ratts, R. Blatnik, L. N. Lee, S. Fischer, L. Borkner, J. D. Oduro, T. F. Marandu, S. Hoppe, Z. Ruzsics, et al. 2016. Peptide processing is critical for T-cell memory inflation and may be optimized to improve immune protection by CMV-based vaccine vectors. *PLoS Pathog.* 12: e1006072.
7. Karer, U., S. Sierra, M. Wagner, A. Oxenius, H. Hengel, U. H. Koszinowski, R. E. Phillips, and P. Klennerman. 2003. Memory inflation: continuous accumulation of antiviral CD8+ T cells over time. *J. Immunol.* 170: 2022–2029.
8. Munks, M. W., K. S. Cho, A. K. Pinto, S. Sierra, P. Klennerman, and A. B. Hill. 2006. Four distinct patterns of memory CD8 T cell responses to chronic murine cytomegalovirus infection. *J. Immunol.* 177: 450–458.
9. Sierra, S., R. Rothkopf, and P. Klennerman. 2005. Evolution of diverse antiviral CD8+ T cell populations after murine cytomegalovirus infection. *Eur. J. Immunol.* 35: 1113–1123.
10. Burgers, W. A., C. Riou, M. Mlotshwa, P. Maenetje, D. de Assis Rosa, J. Brenchley, K. Mlisana, D. C. Douek, R. Koup, M. Roederer, et al; CAPRISA 002 Acute Infection Study Team. 2009. Association of HIV-specific and total CD8+ T memory phenotypes in subtype C HIV-1 infection with viral set point. *J. Immunol.* 182: 4751–4761.
11. Pachnio, A., M. Ciaurriz, J. Begum, N. Lal, J. Zuo, A. Beggs, and P. Moss. 2016. Cytomegalovirus infection leads to development of high frequencies of cytotoxic virus-specific CD4+ T cells targeted to vascular endothelium. *PLoS Pathog.* 12: e1005832.
12. Snyder, C. M., K. S. Cho, E. L. Bonnett, S. van Dommelen, G. R. Shellam, and A. B. Hill. 2008. Memory inflation during chronic viral infection is maintained by continuous production of short-lived, functional T cells. *Immunity* 29: 650–659.
13. Conrad, J. A., R. K. Ramalingam, R. M. Smith, L. Barnett, S. L. Lorey, J. Wei, B. C. Simons, S. Sadagopal, D. Meyer-Olson, and S. A. Kalams. 2011. Dominant clonotypes within HIV-specific T cell responses are programmed death-1high and CD127low and display reduced variant cross-reactivity. *J. Immunol.* 186: 6871–6885.
14. O'Hara, G. A., S. P. Welten, P. Klennerman, and R. Arens. 2012. Memory T cell inflation: understanding cause and effect. *Trends Immunol.* 33: 84–90.
15. Okoye, A. A., M. Rohankhedkar, A. L. Konfe, C. O. Abana, M. D. Reyes, J. A. Clock, D. M. Duell, A. W. Sylvester, P. Sammader, A. W. Legasse, et al. 2015. Effect of IL-7 therapy on naïve and memory T cell homeostasis in aged rhesus macaques. *J. Immunol.* 195: 4292–4305.
16. Johnston, R. J., L. Comps-Agrar, J. Hackney, X. Yu, M. Huseni, Y. Yang, S. Park, V. Javinal, H. Chiu, B. Irving, et al. 2014. The immunoreceptor TIGIT regulates antitumor and antiviral CD8(+) T cell effector function. *Cancer Cell* 26: 923–937.
17. Gamadia, L. E., E. M. van Leeuwen, E. B. Remmerswaal, S. L. Yong, S. Surachno, P. M. Wertheim-van Dillen, I. J. Ten Berge, and R. A. Van Lier. 2004. The size and phenotype of virus-specific T cell populations is determined by repetitive antigenic stimulation and environmental cytokines. *J. Immunol.* 172: 6107–6114.
18. Klennerman, P., and A. Hill. 2005. T cells and viral persistence: lessons from diverse infections. *Nat. Immunol.* 6: 873–879.
19. Lang, A., J. D. Brien, and J. Nikolich-Zugich. 2009. Inflation and long-term maintenance of CD8 T cells responding to a latent herpesvirus depend upon establishment of latency and presence of viral antigens. *J. Immunol.* 183: 8077–8087.
20. Holtappels, R., M. F. Pahl-Seibert, D. Thomas, and M. J. Reddehase. 2000. Enrichment of immediate-early 1 (m123/pp89) peptide-specific CD8 T cells in a pulmonary CD62L(lo) memory-effector cell pool during latent murine cytomegalovirus infection of the lungs. *J. Virol.* 74: 11495–11503.
21. Seckert, C. K., M. Griessl, J. K. Büttner, S. Scheller, C. O. Simon, K. A. Kropp, A. Renzaho, B. Kühnapfel, N. K. Grzimek, and M. J. Reddehase. 2012. Viral latency drives ‘memory inflation’: a unifying hypothesis linking two hallmarks of cytomegalovirus infection. *Med. Microbiol. Immunol.* 201: 551–566.
22. Simon, C. O., R. Holtappels, H. M. Tervo, V. Böhml, T. Däubner, S. A. Oehrlein-Karpi, B. Kühnapfel, A. Renzaho, D. Strand, J. Podlech, et al. 2006. CD8 T cells control cytomegalovirus latency by epitope-specific sensing of transcriptional reactivation. *J. Virol.* 80: 10436–10456.
23. Seckert, C. K., S. I. Schader, S. Ebert, D. Thomas, K. Freitag, A. Renzaho, J. Podlech, M. J. Reddehase, and R. Holtappels. 2011. Antigen-presenting cells of haematopoietic origin prime cytomegalovirus-specific CD8 T-cells but are not sufficient for driving memory inflation during viral latency. *J. Gen. Virol.* 92: 1994–2005.
24. Torti, N., S. M. Walton, T. Brocker, T. Rülicke, and A. Oxenius. 2011. Non-hematopoietic cells in lymph nodes drive memory CD8 T cell inflation during murine cytomegalovirus infection. *PLoS Pathog.* 7: e1002313.
25. Gordon, C. L., M. Miron, J. J. Thome, N. Matsuoka, J. Weiner, M. A. Rak, S. Igarashi, T. Granot, H. Lerner, F. Goodrum, and D. L. Farber. 2017. Tissue reservoirs of antiviral T cell immunity in persistent human CMV infection. *J. Exp. Med.* 214: 651–667.
26. O'Bryan, J. M., M. Woda, M. Co, A. Mathew, and A. L. Rothman. 2013. Telomere length dynamics in human memory T cells specific for viruses causing acute or latent infections. *Immun. Ageing* 10: 37.
27. Hutchinson, S., S. Sims, G. O'Hara, J. Silk, U. Gileadi, V. Cerundolo, and P. Klennerman. 2011. A dominant role for the immunoproteasome in CD8+ T cell responses to murine cytomegalovirus. *PLoS One* 6: e14646.
28. Hegde, N. R., C. Dunn, D. M. Lewinsohn, M. A. Jarvis, J. A. Nelson, and D. C. Johnson. 2005. Endogenous human cytomegalovirus gB is presented efficiently by MHC class II molecules to CD4+ CTL. *J. Exp. Med.* 202: 1109–1119.
29. Walton, S. M., N. Torti, S. Mandaric, and A. Oxenius. 2011. T-cell help permits memory CD8(+) T-cell inflation during cytomegalovirus latency. *Eur. J. Immunol.* 41: 2248–2259.
30. Komanduri, K. V., S. M. Donahoe, W. J. Moretto, D. K. Schmidt, G. Gillespie, G. S. Ogg, M. Roederer, D. F. Nixon, and J. M. McCune. 2001. Direct measurement of CD4+ and CD8+ T-cell responses to CMV in HIV-1-infected subjects. *Virology* 279: 459–470.
31. Lichtner, M., P. Cicconi, S. Vita, A. Cozzi-Lepri, M. Galli, S. Lo Caputo, A. Saracino, A. De Luca, M. Moioli, F. Maggiolo, et al; ICONA Foundation Study. 2015. Cytomegalovirus coinfection is associated with an increased risk of severe non-AIDS-defining events in a large cohort of HIV-infected patients. *J. Infect. Dis.* 211: 178–186.
32. Maidji, E., M. Somsouk, J. M. Rivera, P. W. Hunt, and C. A. Stoddart. 2017. Replication of CMV in the gut of HIV-infected individuals and epithelial barrier dysfunction. *PLoS Pathog.* 13: e1006202.
33. Sylvester, A. W., B. L. Mitchell, J. B. Edgar, C. Taormina, C. Pelte, F. Ruchti, P. R. Sleath, K. H. Grabstein, N. A. Hosken, F. Kern, et al. 2005. Broadly targeted human cytomegalovirus-specific CD4+ and CD8+ T cells dominate the memory compartments of exposed subjects. *J. Exp. Med.* 202: 673–685.
34. Kambayashi, T., and T. M. Laufer. 2014. Atypical MHC class II-expressing antigen-presenting cells: can anything replace a dendritic cell? *Nat. Rev. Immunol.* 14: 719–730.
35. Pachnio, A., J. Zuo, G. B. Ryan, J. Begum, and P. A. Moss. 2015. The cellular localization of human cytomegalovirus glycoprotein expression greatly influences the frequency and functional phenotype of specific CD4+ T cell responses. *J. Immunol.* 195: 3803–3815.
36. Broadley, I., A. Pera, G. Morrow, K. A. Davies, and F. Kern. 2017. Expansions of cytotoxic CD4(+)CD28(−) T cells drive excess cardiovascular mortality in rheumatoid arthritis and other chronic inflammatory conditions and are triggered by CMV infection. *Front. Immunol.* 8: 195.
37. Walker, J. D., C. L. Maier, and J. S. Pober. 2009. Cytomegalovirus-infected human endothelial cells can stimulate allogeneic CD4+ memory T cells by releasing antigenic exosomes. *J. Immunol.* 182: 1548–1559.
38. Elkington, R., N. H. Shoukry, S. Walker, T. Crough, C. Fazou, A. Kaur, C. M. Walker, and R. Khanna. 2004. Cross-reactive recognition of human and primate cytomegalovirus sequences by human CD4 cytotoxic T lymphocytes specific for glycoprotein B and H. *Eur. J. Immunol.* 34: 3216–3226.
39. Barbaro, G., S. D. Fisher, and S. E. Lipshultz. 2001. Pathogenesis of HIV-associated cardiovascular complications. *Lancet Infect. Dis.* 1: 115–124.
40. Hsue, P. Y., J. C. Lo, A. Franklin, A. F. Bolger, J. N. Martin, S. G. Deeks, and D. D. Waters. 2004. Progression of atherosclerosis as assessed by carotid intima-media thickness in patients with HIV infection. *Circulation* 109: 1603–1608.
41. Cheng, J., Q. Ke, Z. Jin, H. Wang, O. Kocher, J. P. Morgan, J. Zhang, and C. S. Crumpacker. 2009. Cytomegalovirus infection causes an increase of arterial blood pressure. *PLoS Pathog.* 5: e1000427.
42. Wall, N. A., C. D. Chue, N. C. Edwards, T. Pankhurst, L. Harper, R. P. Steeds, S. Lauder, J. N. Townend, P. Moss, and C. J. Ferro. 2013. Cytomegalovirus seropositivity is associated with increased arterial stiffness in patients with chronic kidney disease. *PLoS One* 8: e55686.
43. Slot, M. C., A. A. Kroon, J. G. Damoiseaux, R. Theunissen, A. J. Houben, P. W. de Leeuw, and J. W. Tervaert. 2017. CD4(+)CD28(null) T cells are related to previous cytomegalovirus infection but not to accelerated atherosclerosis in ANCA-associated vasculitis. *Rheumatol. Int.* 37: 791–798.
44. Kaplan, R. C., E. Sinclair, A. L. Landay, N. Lurain, A. R. Sharrett, S. J. Gange, X. Xue, P. Hunt, R. Karim, D. M. Kern, et al. 2011. T cell activation and senescence predict subclinical carotid artery disease in HIV-infected women. *J. Infect. Dis.* 203: 452–463.
45. Smith, M. Z., S. Bastidas, U. Karrer, and A. Oxenius. 2013. Impact of antigen specificity on CD4+ T cell activation in chronic HIV-1 infection. *BMC Infect. Dis.* 13: 100.
46. Hunt, P. W., J. N. Martin, E. Sinclair, L. Epling, J. Teague, M. A. Jacobson, R. P. Tracy, L. Corey, and S. G. Deeks. 2011. Valganciclovir reduces T cell activation in HIV-infected individuals with incomplete CD4+ T cell recovery on antiretroviral therapy. *J. Infect. Dis.* 203: 1474–1483.
47. Sacre, K., P. W. Hunt, P. Y. Hsue, E. Maidji, J. N. Martin, S. G. Deeks, B. Autran, and J. M. McCune. 2012. A role for cytomegalovirus-specific CD4+CX3CR1+ T cells and cytomegalovirus-induced T-cell immunopathology in HIV-associated atherosclerosis. *AIDS* 26: 805–814.

48. van de Berg, P. J., S. L. Yong, E. B. Remmerswaal, R. A. van Lier, and I. J. ten Berge. 2012. Cytomegalovirus-induced effector T cells cause endothelial cell damage. *Clin. Vaccine Immunol.* 19: 772–779.
49. Chanouzas, D., L. Dyall, J. Dale, P. Moss, M. Morgan, and L. Harper. 2015. CD4+CD28-T cell expansions in ANCA-associated vasculitis and association with arterial stiffness: baseline data from a randomised controlled trial. *Lancet* 385(Suppl. 1): S30.
50. Chanouzas, D., M. Sagmeister, L. Dyall, P. Nightingale, C. Ferro, P. Moss, M. Morgan, and L. Harper. 2017. Role of cytomegalovirus in the expansion of CD4+CD28-T cells in patients with ANCA-associated vasculitis: a proof-of-concept, randomised controlled trial. *Lancet* 389: S17.
51. Klennerman, P., V. Cerundolo, and P. R. Dunbar. 2002. Tracking T cells with tetramers: new tales from new tools. *Nat. Rev. Immunol.* 2: 263–272.
52. Nicholas, K. J., D. K. Flaherty, R. M. Smith, D. N. Sather, and S. A. Kalams. 2017. Chronic HIV-1 infection impairs superantigen-induced activation of peripheral CD4+CXCR5+PD-1+ cells, with relative preservation of recall antigen-specific responses. *J. Acquir. Immune Defic. Syndr.* 74: 72–80.
53. Li Pira, G., L. Bottone, F. Ivaldi, R. Pelizzoli, F. Del Galdo, L. Lozzi, L. Bracci, A. Loregian, G. Palù, R. De Palma, et al. 2004. Identification of new Th peptides from the cytomegalovirus protein pp65 to design a peptide library for generation of CD4 T cell lines for cellular immunoreconstitution. *Int. Immunol.* 16: 635–642.
54. James, E. A., J. Bui, D. Berger, L. Huston, M. Roti, and W. W. Kwok. 2007. Tetramer-guided epitope mapping reveals broad, individualized repertoires of tetanus toxin-specific CD4+ T cells and suggests HLA-based differences in epitope recognition. *Int. Immunol.* 19: 1291–1301.
55. Vingert, B., S. Perez-Patridgeon, P. Jeannin, O. Lambotte, F. Boufassa, F. Lemaitre, W. W. Kwok, I. Theodorou, J. F. Delfraissy, J. Thèze, and L. A. Chakrabarti, ANRS EP36 HIV Controllers Study Group. 2010. HIV controller CD4+ T cells respond to minimal amounts of Gag antigen due to high TCR avidity. *PLoS Pathog.* 6: e1000780.
56. Long, H. M., O. L. Chagoury, A. M. Leese, G. B. Ryan, E. James, L. T. Morton, R. J. Abbott, S. Sabbah, W. Kwok, and A. B. Rickinson. 2013. MHC II tetramers visualize human CD4+ T cell responses to Epstein-Barr virus infection and demonstrate atypical kinetics of the nuclear antigen EBNA1 response. *J. Exp. Med.* 210: 933–949.
57. Leisner, C., N. Loeth, K. Lamberth, S. Justesen, C. Sylvester-Hvid, E. G. Schmidt, M. Claesson, S. Buus, and A. Stryhn. 2008. One-pot, mix-and-read peptide-MHC tetramers. *PLoS One* 3: e1678.
58. Gu, Z., L. Gu, R. Eils, M. Schlesner, and B. Brors. 2014. circlize implements and enhances circular visualization in R. *Bioinformatics* 30: 2811–2812.
59. Shugay, M., D. V. Bagaev, M. A. Turchaninova, D. A. Bolotin, O. V. Britanova, E. V. Putintseva, M. V. Pogorely, V. I. Nazarov, I. V. Zvyagin, V. I. Kirgizova, et al. 2015. VDItools: unifying post-analysis of T cell receptor repertoires. *PLOS Comput. Biol.* 11: e1004503.
60. Han, A., J. Glanville, L. Hansmann, and M. M. Davis. 2014. Linking T-cell receptor sequence to functional phenotype at the single-cell level. *Nat. Biotechnol.* 32: 684–692.
61. Anmole, G., X. T. Kuang, M. Toyoda, E. Martin, A. Shahid, A. Q. Le, T. Markle, B. Baraki, R. B. Jones, M. A. Ostrowski, et al. 2015. A robust and scalable TCR-based reporter cell assay to measure HIV-1 Nef-mediated T cell immune evasion. *J. Immunol. Methods* 426: 104–113.
62. Strain, M. C., S. M. Lada, T. Luong, S. E. Rought, S. Gianella, V. H. Terry, C. A. Spina, C. H. Woell, and D. D. Richman. 2013. Highly precise measurement of HIV DNA by droplet digital PCR. *PLoS One* 8: e55943.
63. Garg, A., R. Trout, and S. A. Spector. 2017. Human immunodeficiency virus type-1 myeloid derived suppressor cells inhibit cytomegalovirus inflammation through interleukin-27 and B7-H4. *Sci. Rep.* 7: 44485.
64. Crompton, L., N. Khan, R. Khanna, L. Nayak, and P. A. Moss. 2008. CD4+ T cells specific for glycoprotein B from cytomegalovirus exhibit extreme conservation of T-cell receptor usage between different individuals. *Blood* 111: 2053–2061.
65. Ventura, C., H. Bisceglia, Y. Girerd-Chambaz, N. Burdin, and P. Chaux. 2012. HLA-DR and HLA-DP restricted epitopes from human cytomegalovirus glycoprotein B recognized by CD4+ T-cell clones from chronically infected individuals. *J. Clin. Immunol.* 32: 1305–1316.
66. Brenchley, J. M., N. J. Karandikar, M. R. Betts, D. R. Ambrozak, B. J. Hill, L. E. Crotty, J. P. Casazza, J. Kuruppu, S. A. Migueles, M. Connors, et al. 2003. Expression of CD57 defines replicative senescence and antigen-induced apoptotic death of CD8+ T cells. *Blood* 101: 2711–2720.
67. Acierno, P. M., D. A. Newton, E. A. Brown, L. A. Maes, J. E. Baatz, and S. Gattoni-Celli. 2003. Cross-reactivity between HLA-A2-restricted FLU-M1: 58–66 and HIV p17 GAG:77–85 epitopes in HIV-infected and uninfected individuals. *J. Transl. Med.* 1: 3.
68. Chattopadhyay, P. K., and M. Roederer. 2010. Good cell, bad cell: flow cytometry reveals T-cell subsets important in HIV disease. *Cytometry A* 77: 614–622.
69. Smuda, C., E. Bogner, and K. Radsak. 1997. The human cytomegalovirus glycoprotein B gene (ORF UL55) is expressed early in the infectious cycle. *J. Gen. Virol.* 78: 1981–1992.
70. Dekhtarenko, I., M. A. Jarvis, Z. Ruzsics, and L. Čicin-Šain. 2013. The context of gene expression defines the immunodominance hierarchy of cytomegalovirus antigens. *J. Immunol.* 190: 3399–3409.
71. Appay, V., J. J. Zaunders, L. Papagno, J. Sutton, A. Jaramillo, A. Waters, P. Easterbrook, P. Grey, D. Smith, A. J. McMichael, et al. 2002. Characterization of CD4(+) CTLs ex vivo. *J. Immunol.* 168: 5954–5958.
72. Oswald-Richter, K., S. M. Grill, M. Leelawong, M. Tseng, S. A. Kalams, T. Hulgat, D. W. Haas, and D. Unutmaz. 2007. Identification of a CCR5-expressing T cell subset that is resistant to R5-tropic HIV infection. *PLoS Pathog.* 3: e58.
73. Ertelt, J. M., T. M. Johanns, M. A. Mysz, M. R. Nanton, J. H. Rowe, M. N. Aguilera, and S. S. Way. 2011. Selective culling of high avidity antigen-specific CD4+ T cells after virulent *Salmonella* infection. *Immunology* 134: 487–497.
74. Falta, M. T., A. P. Fontenot, E. F. Rosloniec, F. Crawford, C. L. Roark, J. Bill, P. Marrack, J. Kappler, and B. L. Kotzin. 2005. Class II major histocompatibility complex-peptide tetramer staining in relation to functional avidity and T cell receptor diversity in the mouse CD4(+) T cell response to a rheumatoid arthritis-associated antigen. *Arthritis Rheum.* 52: 1885–1896.
75. Kim, C., T. Wilson, K. F. Fischer, and M. A. Williams. 2013. Sustained interactions between T cell receptors and antigens promote the differentiation of CD4+ memory T cells. *Immunity* 39: 508–520.
76. Kimata, M., D. L. Cullins, M. L. Brown, D. D. Brand, E. F. Rosloniec, L. K. Myers, J. M. Stuart, and A. H. Kang. 2012. Characterization of inhibitory T cells induced by an analog of type II collagen in an HLA-DR1 humanized mouse model of autoimmune arthritis. *Arthritis Res. Ther.* 14: R107.
77. Koehne, G., A. Hasan, E. Doubrovina, S. Prokopenko, E. Tyler, G. Wasilewski, and R. J. O'Reilly. 2015. Immunotherapy with donor T cells sensitized with overlapping pentadecapeptides for treatment of persistent cytomegalovirus infection or viremia. *Biol. Blood Marrow Transplant.* 21: 1663–1678.
78. Lanzer, K. G., L. L. Johnson, D. L. Woodland, and M. A. Blackman. 2014. Impact of ageing on the response and repertoire of influenza virus-specific CD4 T cells. *Immun. Ageing* 11: 9.
79. Legoux, F., L. Gautreau, L. Hesnard, A. Leger, M. Moyon, M. C. Devilder, M. Bonneville, and X. Saulquin. 2013. Characterization of the human CD4(+) T-cell repertoire specific for major histocompatibility class I-restricted antigens. *Eur. J. Immunol.* 43: 3244–3253.
80. Nose, H., R. Kubota, N. P. Seth, P. K. Goon, Y. Tanaka, S. Izumo, K. Usuku, Y. Ohara, K. W. Wucherpfennig, C. R. Bangham, et al. 2007. Ex vivo analysis of human T lymphotropic virus type 1-specific CD4+ cells by use of a major histocompatibility complex class II tetramer composed of a neurological disease-susceptibility allele and its immunodominant peptide. *J. Infect. Dis.* 196: 1761–1772.
81. Petersen, J., J. van Bergen, K. L. Loh, Y. Kooy-Winkelaar, D. X. Beringer, A. Thompson, S. F. Bakker, C. J. Mulder, K. Ladell, J. E. McLaren, et al. 2015. Determinants of gliadin-specific T cell selection in celiac disease. *J. Immunol.* 194: 6112–6122.
82. Poli, C., C. Raffin, D. Dojcinovic, I. Luescher, M. Ayyoub, and D. Valmori. 2013. MHC class II/ESO tetramer-based generation of in vitro primed anti-tumor T-helper lines for adoptive cell therapy of cancer. *Haematologica* 98: 316–322.
83. Sabatino Jr., J. J., J. Huang, C. Zhu, and B. D. Avavold. 2011. High prevalence of low affinity peptide-MHC II tetramer-negative effectors during polyclonal CD4+ T cell responses. *J. Exp. Med.* 208: 81–90.
84. Braendstrup, P., B. K. Mortensen, S. Justesen, T. Osterby, M. Rasmussen, A. M. Hansen, C. B. Christiansen, M. B. Hansen, M. Nielsen, L. Vindeløv, et al. 2014. Identification and HLA-tetramer-validation of human CD4+ and CD8+ T cell responses against HCMV proteins IE1 and IE2. *PLoS One* 9: e94892.
85. Glanville, J., H. Huang, A. Nau, O. Hatton, L. E. Wagar, F. Rubelt, X. Ji, A. Han, S. M. Krams, C. Pettus, et al. 2017. Identifying specificity groups in the T cell receptor repertoire. *Nature* 547: 94–98.
86. Hui, E., J. Cheung, J. Zhu, X. Su, M. J. Taylor, H. A. Wallweber, D. K. Sasmal, J. Huang, J. M. Kim, I. Mellman, and R. D. Vale. 2017. T cell costimulatory receptor CD28 is a primary target for PD-1-mediated inhibition. *Science* 355: 1428–1433.
87. Kamphorst, A. O., A. Wieland, T. Nasti, S. Yang, R. Zhang, D. L. Barber, B. T. Konieczny, C. Z. Daugherty, L. Koenig, K. Yu, et al. 2017. Rescue of exhausted CD8+ T cells by PD-1-targeted therapies is CD28-dependent. *Science* 355: 1423–1427.
88. Okoye, A. A., M. Rohankhedkar, C. Abana, A. Pattenn, M. Reyes, C. Pexton, R. Lum, A. Sylwestre, S. L. Planer, A. Legasse, et al. 2012. Naïve T cells are dispensable for memory CD4+ T cell homeostasis in progressive simian immunodeficiency virus infection. *J. Exp. Med.* 209: 641–651.

Supplemental data

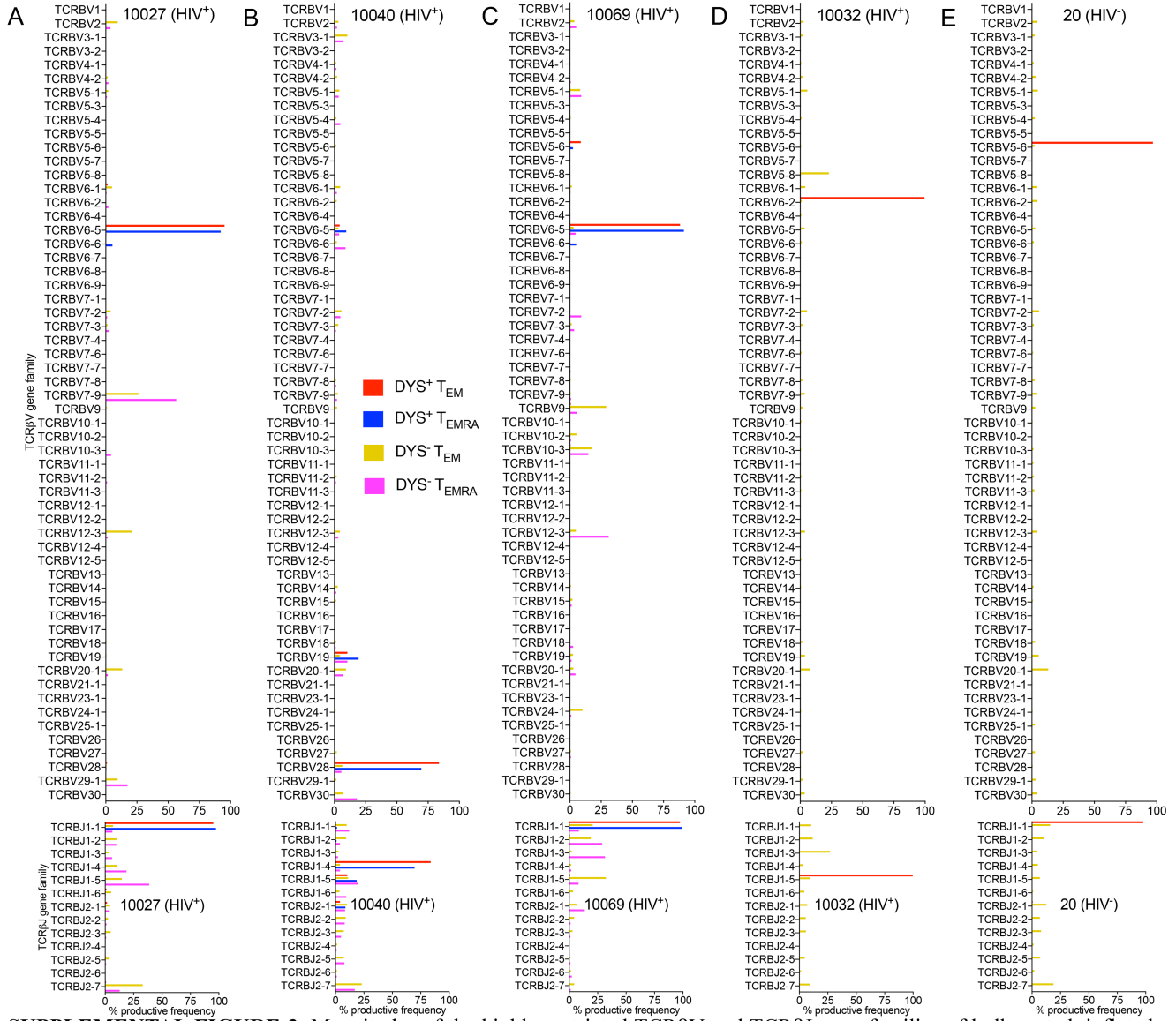


SUPPLEMENTAL FIGURE 1. Representative gating hierarchy for CD4⁺ T cell tetramer staining. FlowJo plots were obtained from CD4-enriched PBMCs of subject 10027's tp2 using PE-conjugated DR7:DYS tetramer. DYS- and DYS+: DYS- and DYS⁺ CD4⁺ T cells, respectively; CM+, TM+, and EM+: central, transitional and effector memory T cells, respectively; Nai+, Int+ and TEMRA+: naïve, intermediate and T-effector memory-RA⁺ T cells, respectively. Data represent ten biological replicates. The CD4 vs. DR7:DYS tetramer (PE) plot is also shown in fig. 1B.

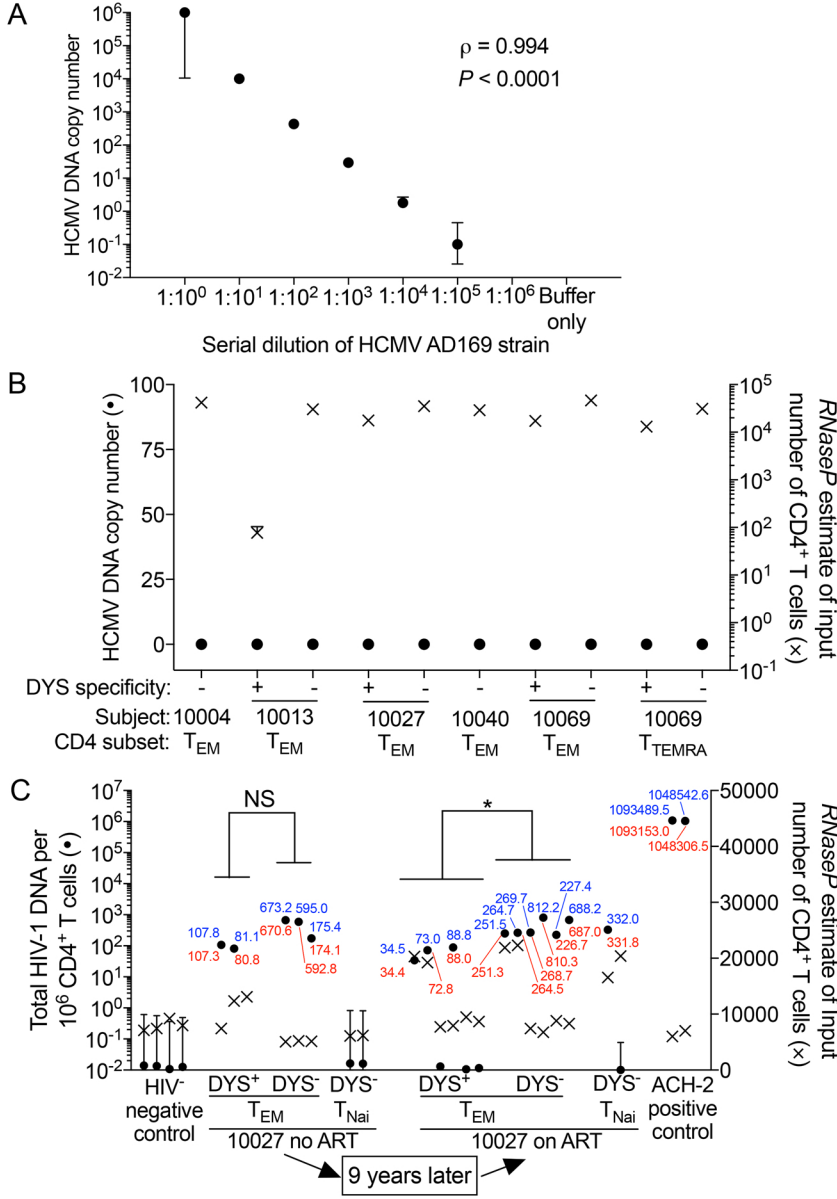


SUPPLEMENTAL FIGURE 2. DYS⁺ CD4⁺ T cell responses are dependent on HLA-DR7 allele, and other DR7⁺ epitope-specific CD4⁺ T cells are present at low magnitudes in HIV⁺ DR7⁺ subjects. (A) DYS ($n=7$) and (B) EPD ($n=5$) tetramer stains of HIV⁺ DR7⁻ subjects representing single experiments. EPD tetramer stain of PBMCs from (C) HIV⁺ DR7⁺ ($n=8$) and (D) HIV⁻ DR7⁺ ($n=10$) subjects. (E)

Response magnitude comparisons of DR7-restricted CD4⁺ T cells from the HIV⁺ HCMV⁺ DR7⁺ cohort that are specific for DYS, tetanus toxoid precursor LIN, EBV EBNA2 PRS or HIV gag FRD epitopes ($n=8$; tp1 of Subject 10004, and tp2 of Subjects 10013, 10027 and 10032). (F) CD8 A2:NLV tetramer stain of Subject 10027's tp2 PBMCs. Data represent at least two biological replicates except Subject 10032's EPD tetramer stain due to insufficient cells and panel (E). PBMCs were CD4-enriched or left untouched. ** $p \leq 0.01$.



SUPPLEMENTAL FIGURE 3. Magnitudes of the highly restricted TCR β V and TCR β J gene families of bulk-sorted, inflated DYS⁺ CD4⁺ T cells. Data represent single experiments for Subjects (A) 10027, (B) 10040, (C) 10069, (D) 10032, and (E) 20, which complement fig. 3. Top row: TCR β V; bottom row: TCR β J.



SUPPLEMENTAL FIGURE 4. Inflated DYS⁺ CD4⁺ T cells serve as latent HIV but not HCMV reservoirs. **A–B:** Droplet digital PCR (ddPCR) HCMV DNA quantitation in single experiments of (A) HCMV AD169 strain serial dilutions, and (B) DYS⁺ and DYS⁻ CD4⁺ T cells from HIV⁺ HCMV⁺ DR7⁺ subjects ($n=6$). (C) ddPCR HIV DNA quantitation comparison between DYS⁺ and DYS⁻ CD4⁺ T_{EM} from Subject 10027's tp1 (no ART) and tp2 (on ART). Blue and red numbers: upper and lower 95% CI, respectively. Data represent 3 technical replicates except tp2 with two biological replicates containing 3 technical replicates each. Data points at 10⁻¹ indicate undetected HIV DNA. **B–C:** Left y-axis: HCMV or HIV genome copy number after normalization with RNaseP housekeeping gene. Right y-axis: input number of cells, which was determined by dividing the RNaseP concentration (in g/ μ l) in the PCR volume by 2 (because there are two copies of RNaseP per cell) and multiplying by the total ddPCR volume (20 μ l). This product is divided by the standard number of DNA per cell (6 pg/cell) to determine the input number of cells per reaction. Both graphs show 95% CI determined from the concentration ratio of HCMV IE1+IE2 (B) or HIV gag (C) to RNaseP \pm 1.96 times the standard error ratio of the concentration ratios. * $p \leq 0.05$.